Synthesis, Properties, and Ceramic Conversion Reactions of Polyborazylene. A High-Yield Polymeric Precursor to Boron Nitride

Paul J. Fazen,[1] Edward E. Remsen,*[,2] Jeffrey S. Beck,[3] Patrick J. Carroll,[1] Andrew R. McGhie,[1] and Larry G. Sneddon*[,1]

Department of Chemistry and Laboratory for Research on the Structure of Matter, University of Pennsylvania, Philadelphia, Pennsylvania 19104-6323 and Analytical Sciences Center, Monsanto Corporate Research, Monsanto Company, 800 N. Lindbergh Boulevard, St. Louis, Missouri 63167

Received May 23, 1995. Revised Manuscript Received August 15, 1995[⊗]

Borazine readily dehydropolymerizes at moderate temperatures (70–110 °C) to give a soluble polymer, polyborazylene, in excellent yields of 81–91%. The polymer is isolated as a white solid that is soluble in ethers such as glyme and THF. The polymer can be precipitated by slowly adding ether solutions of the polymer to pentane. Elemental analysis indicates that compositions range from $B_3N_3H_{3.4}$ to $B_3N_3H_{3.9}$ for crude polymers and from $B_3N_3H_{2.65}$ to $B_3N_3H_{3.8}$ for precipitated samples, with average empirical formulas of $B_3N_{3.1}H_{3.6}$ and $B_3N_{3.1}H_{3.4}$, respectively. Diffuse reflectance infrared Fourier transform (DRIFT) and ^{11}B NMR spectra indicate that the borazine ring structure is retained in the polymer. Powder X-ray diffraction suggests the presence of a layered structure for the polymer in the solid state, which is consistent with its observed density of 1.5–1.6 g/cm^3. Molecular weight studies using size exclusion chromatography (SEC)/viscometric detection (VISC) give accurate determinations of a lower value of M_n, 500–900 g/mol. SEC/low-angle laser light scattering (LALLS)/ultraviolet absorbance (UV) give determinations of M_w biased toward high molecular weights, with values usually between 3000 and 8000 g/mol. The combined spectroscopic and molecular weight data indicate that the polymer appears to have a complex structure, having linear, branched-chain and fused-cyclic segments, related to those of the organic polyphenylenes. The isolation and X-ray structural characterizations of small amounts of the polycyclic boron–nitrogen compounds diborazine, 1:2′-$(B_3N_3H_5)_2$, and borazanaphthalene, $B_5N_5H_8$, supports this conclusion and provide models for the primary structural units of the polymer. Pyrolysis studies show that the polymer converts to boron nitride in excellent chemical, 89–99%, and ceramic yields, 84–93%. The quality of the resulting boron nitride was determined by elemental analysis, DRIFT spectra, powder XRD, density measurements, and TGA oxidation studies. Solutions of polyborazylene were also used to coat carbon and ceramic fiber yarn bundles, which, when pyrolyzed under argon or ammonia, produced excellent boron nitride coatings as characterized by AES spectroscopy. Studies of the polymer/ceramic conversion process, as followed by TGA, TGA/MS, DRIFT, XRD, and microanalysis of materials produced at intermediate temperatures, suggest that the polymer converts to boron nitride by means of a two-dimensional cross-linking reaction. Alkyl-substituted polyborazylenes were produced by either the polymerization of *B*-alkylborazines or by the transition-metal catalyzed hydroboration of olefins by the parent polyborazylene. The alkylated polyborazylenes were found to have greatly increased solubilities in organic solvents. In addition, studies of their ceramic conversion reactions showed that polymer cross-linking was inhibited, with the initial weight losses occurring at slightly higher temperatures than in the parent polymers.

Introduction

Interest in boron containing polymers has been stimulated by the search for processible precursors to boron nitride ceramics.[4] Borazine-based polymers offer a number of advantages as precursor materials. However, many of the known borazine-based preceramic polymers are not meltable, processible, or soluble in organic solvents or contain too much carbon to produce high-quality boron nitride. Therefore, there is a clear need to develop processible, soluble borazine-based polymers with minimal carbon content.

Polyborazylene[5] polymers, such as shown below, composed of linked borazine rings analogous to the

[⊗] Abstract published in *Advance ACS Abstracts*, September 15, 1995.

(1) University of Pennsylvania.

(2) Monsanto Corporate Research.

(3) Current address: Mobil Research and Development, P.O. Box 480, Paulsboro, NJ 08066.

(4) (a) Paine, R. T.; Narula, C. K. *Chem. Rev.* **1990**, *90*, 73–91. (b) Paine, R. T.; Sneddon, L. G. In *Inorganic and Organometallic Polymers*; Wisian-Neilson, P., Allcock, H. R., Wynne, K. J., Eds.; ACS Symposium Series; American Chemical Society: Washington, DC, 1994; pp 358–374. (c) Kimura, Y.; Kubo, Yoshiteru, K. in *Inorganic and Organometallic Polymers*; Wisian-Neilson, P.; Allcock, H. R.; Wynne, K. J.; Eds.; ACS Symposium Series; American Chemical Society: Washington, DC, 1994, pp 375–388.

(5) The alternative IUPAC approved name for this homopolymer would be poly(borazinediyl).

0897-4756/95/2807-1942$09.00/0

organic polyphenylene polymers,[6] are of particular interest because of their potentially high ceramic yields (95%) and their close structural relationship to boron nitride. However, at the outset of this work no tractable dehydrocoupled polymers derived from the parent borazine, $B_3N_3H_6$, had been characterized.

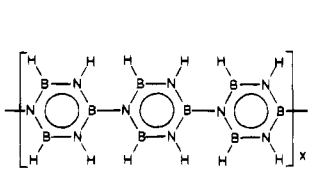

p-polyborazylene

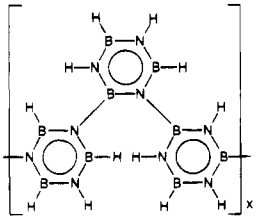

o-polyborazylene

Small dehydrodimers and oligomers of alkylated borazines had previously been prepared. For example, when *B*-trichloroborazines were reacted with Grignard reagents, peralkyldiborazines were reported side products.[7] When *N*-lithiopentaalkylborazine was reacted with *B*-chloropentaalkylborazine, a decaalkyldiborazine was produced in good yields. Polymeric species were also synthesized using *B*-dichloro- and *B*-trichloroperalkylborazines with *N*-lithio- and *N*-dilithioperalkylborazines.[8] More recently, Niedenzu[9] synthesized a number of dimeric and oligomeric alkylated borazine species from the reaction of *B*-dialkyl-*B*-haloborazines with tri-*B*-alkyl-*N*-trimethylsilylated-borazines, $R_3B_3N(SiMe_3)_nH_{3-n}$. Dimeric alkylborazine species have also been synthesized by Wurtz coupling of *B*-chloropentaalkylborazines.[10]

While the above dimeric and oligomeric alkylated borazine species are known, only the B−N coupled dimer 1:2′-$[B_3N_3H_5]_2$ has been obtained from the parent $B_3N_3H_6$ system. Laubengayer[11] and co-workers were the first to isolate small amounts of diborazine, along with borazanaphthalene, $B_5N_5H_8$, and *B*-diaminoborazine $(H_2N)_2B_3N_3H_4$ from the gas-phase pyrolysis of borazine. These compounds were also found as products of the electric discharge[12] or photolysis[13] reactions of borazine. Mamantov also observed mass spectral evidence for diborazine and borazanaphthalene when borazine was allowed to stand at room temperature over a period of 2 months.[14] Other studies of borazine decomposition reactions have reported the formation of white involatile (perhaps polymeric) solids, but these materials were not characterized.[15] In fact, Stock[16] produced an insoluble white solid with an approximate formula of BNH_x, with $x \cong 1$, when he heated borazine to 500 °C.

We have already reported in an initial communication our surprising discovery that *simply heating liquid borazine in vacuo at moderate temperatures* results in a dehydrocoupling reaction to produce a *soluble* borazine polymer in excellent yields.[17] In this paper we report the full details of the synthesis, characterization, and the ceramic conversion reactions of this polyborazylene polymer.

Experimental Section

All manipulations were carried out using standard high-vacuum or inert-atmosphere techniques as described by Shriver.[18]

Materials. Borazine was purchased from Callery Chemical Co. or prepared by a method developed in our labs[19] and purified by vacuum line fractionation through a −45, −78, and −196 °C trap series. The borazine retained in the −78 °C trap was used without further purification. Alkyl-substituted borazines and polyborazylenes were synthesized by methods previously described.[20]

Physical Measurements. ^{1}H NMR spectra at 200.1 MHz and ^{11}B NMR spectra at 64.2 MHz were obtained on a Bruker AF-200 Fourier transform spectrometer. ^{1}H NMR spectra at 500 MHz and ^{11}B NMR spectra at 160.5 MHz were obtained on a Bruker AM-500 Fourier transform spectrometer. The ^{11}B NMR chemical shifts are relative to external $BF_3{\cdot}(C_2H_5)_2$ (0.00 ppm) with a negative sign indicating an upfield shift. Chemical shifts for ^{1}H NMR spectra (ppm) are based on 7.15 ppm for C_6D_6 (relative to Me_4Si at 0.00 ppm). Densities were measured by floatation using halocarbon liquids.

Unit and high-resolution mass spectra were obtained on a VG-Fisons ZAB-E high-resolution mass spectrometer interfaced to a VG 11-250J data system. High-resolution mass spectra were obtained by chemical ionization using either positive or negative ion detection. Gas chromatography/mass spectrometry was performed on a Hewlett-Packard 5890A gas chromatograph (equipped with a cross-linked methylsilicone column) interfaced to a Hewlett-Packard 5970 mass selective detector. Infrared spectra were recorded on a Perkin-Elmer 1430 infrared spectrophotometer. Diffuse reflectance infrared spectra (DRIFT) were obtained on a Perkin-Elmer 7770 Fourier transform spectrophotometer equipped with the appropriate diffuse reflectance attachment. Elemental analyses were performed at Galbraith Laboratories, Knoxville, TN, Nesmeyanov Institute of Organoelement Compounds (INEOS), Moscow, Russia, and Robertson Microlit Laboratories, Inc., Madison, NJ.

Thermogravimetric analyses (TGA) were obtained under argon on either a DuPont 2100 thermal analyzer coupled to a 951 TGA module or a Seiko Model 320 TG/DTA with a heating rates of 10 °C/min. Differential scanning calorimetry (DSC) experiments were carried out under helium with a heating rate of 10 °C/min. A Fisons Thermolab mass spectrometer, having a 1−300 amu mass range, was coupled using a heated capillary interface to the TGA for analysis of evolved gases. Auger electron spectra (AES) were obtained on a Perkin-Elmer Phi 600 scanning microprobe operating at 3 kV primary voltage with a beam current of 0.1 μA, yielding a spot size of ~0.5

(6) (a) Ried, W.; Freitag, D. *Angew. Chem., Int. Ed. Engl.* **1968**, *7*, 835−844. (b) Noren, G. K.; Stille, J. K. *J. Polym. Sci. Part D* **1971**, *5*, 385−430.

(7) (a) Harris, J. J. *J. Org. Chem.* **1961**, *26*, 2155−2156. (b) Meller, A.; Egger, H. *Monatsh. Chem.* **1966**, *97*, 790−791. (c) Meller, A.; Schlegel, R. *Monatsh. Chem.* **1965**, *96*, 1209−1213. (d) Boone, J. L. U. S. Patent 3,317,596, 1967; *Chem. Abstr.* **1967**, *67*, 64514m. (e) Boone, J. L.; Willcockson, G. W. *Inorg. Chem.* **1966**, *5*, 311−313.

(8) Wagner, R. I.; Bradford, J. L. *Inorg. Chem.* **1962**, *1*, 99−106.

(9) Bai, J.; Niedenzu, K.; Serwatowska, J.; Serwatowski J. *Inorg. Chem.* **1992**, *31*, 228−233.

(10) (a) Gutmann, V.; Meller, A.; Schlegel, R. *Monatsh. Chem.* **1964**, *95*, 314−318. (b) Brotherton, R. J.; McCloskey, A. L. U.S. Patent 3,-101,369, 1963; *Chem. Abstr.* **1964**, *60*, 547h.

(11) Laubengayer, A. W.; Moews, P. C., Jr.; Porter, R. F. *J. Am. Chem. Soc.* **1961**, *83*, 1337−1342.

(12) Laubengayer, A. W.; Beachley, O. T., Jr. *Adv. Chem. Ser. No. 42*; American Chemical Society: Washington DC, 1964; pp 281−289.

(13) Neiss, M. A.; Porter, R. F. *J. Am. Chem. Soc.* **1972**, *94*, 1438−1443.

(14) Mamantov, G.; Margrave, J. L. *J. Inorg. Nucl. Chem.* **1961**, *20*, 348−351.

(15) (a) Schaeffer, R.; Steindler, M.; Hohnstedt, L.; Smith, H. S., Jr.; Eddy, L. B.; Schlesinger, H. I. *J. Am. Chem. Soc.* **1954**, *76*, 3303−3306. (b) Haworth, D. T.; Hohnstedt, L. F. *J. Am. Chem. Soc.* **1960**, *82*, 3860−3862.

(16) Stock, A.; Pohland, E. *Chem. Ber.* **1926**, 59, 2215−2223.

(17) (a) Fazen, P. J.; Beck, J. S.; Lynch, A. T.; Remsen, E. E.; Sneddon, L. G. *Chem. Mat.* **1990**, *2*, 96−97. (b) Fazen, P. J.; Remsen, E. E.; Sneddon, L. G. *Polym. Prepr.* **1991**, *32*, 544−545.

(18) Shriver, D. F.; Drezdzon, M. A. *Manipulations of Air Sensitive Compounds*, 2nd ed.; Wiley: New York, 1986.

(19) Wideman, T.; Sneddon, L. G. *Inorg. Chem.* **1995**, *34*, 1002−1003.

(20) Fazen, P. J.; Sneddon, L. G. *Organometallics* **1994**, *13*, 2867−2877.

Table 1. Polymer Synthesis Summary

polymer	reaction time, temp	analysis	empirical formula	M_n	M_w	M_w/M_n
I	48 h, 70 °C	B 40.39, N 52.64, H 4.22, C <0.5	$B_3N_{3.02}H_{3.36}$	506	1467	2.90
I[a]	48 h, 70 °C	B 39.62, N 56.51, H 4.15, C <0.5	$B_{2.7}N_{3.0}H_{3.0}$	1400	4000	2.86
I	48 h, 70 °C	B 39.61, N 51.24, H 4.59, C <0.5	$B_{3.0}N_{3.0}H_{3.72}$			
I	48 h, 70 °C	B 42.28, N 53.43, H 4.69, C 0.22	$B_{3.0}N_{2.92}H_{3.56}$			
I	48 h, 70 °C	B 41.70, H 54.66, H 4.64, C <0.5	$B_{3.0}N_{3.03}H_{3.58}$			
I	48 h, 70 °C	B 41.85, N 54.39, H 4.66, C <0.5	$B_{3.0}N_{3.01}H_{3.58}$			
II	48 h, 70 °C	B 40.74, N 53.80, H 4.10, C <0.5	$B_3N_{3.06}H_{3.25}$	637	1554	2.44
II[a]	48 h, 70 °C	B 42.33, N 53.25, H 3.49, C 1.09	$B_{3.1}N_{3.0}H_{2.7}$	3400	7600	2.23
II	48 h, 70 °C	B 36.13, N 53.49, H 4.62, C 1.85	$B_{3.0}N_{3.18}H_{3.82}$			
II	48 h, 70 °C	B 39.45, N 53.35, H 4.6, C 0.47	$B_3N_{3.13}H_{3.75}$			
III	48 h, 70 °C	B 40.9, N 54.04, H 4.96, C <0.2	$B_3N_{3.06}H_{3.90}$	842	2073	2.46
IV	36 h, 70 °C	B 40.4, N 54.19, H 5.00, C <0.2	$B_3N_{3.11}H_{3.98}$	578	1139	1.97
V[a]	22 h, 70 °C	B 39.9, N 54.07, H 5.13, C <0.5	$B_3N_{3.14}H_{4.14}$	980	2100	2.14
VI	9 h, 110 °C	B 39.82, N 55.13, H, 4,47, C 1.43	$B_3N_{3.21}H_{3.61}$	580	2026	3.50
VII	114 h, 70 °C (toluene)	B 40.71, N, 53.97, H 4.66, C 1.15	$B_3N_{3.06}H_{3.68}$	849	3158	3.72
VIII	135 h, 70 °C (benzene)			223	472	2.12
IX	216 h, 70 °C (glyme)			561	16,700	29.8
X[a]	6 days, 90 °C	B 32.37, N 43.45, H, 6.05, C 16.81	$B_3N_{3.1}H_{2.5}(C_2H_5)_{0.7}$	786	3200	4.07
XI	28 days, 70 °C	B28.9, N 40.82, H 7.02, C 20.80	$B_3N_{3.5}H_{3.0}(C_2H_5)_{1.0}$	540	926	1.71
XII	28 days, 70 °C	B 27.8, N 35.26, H 8.04, C 29.20	$B_3N_{2.9}H_{2.7}(C_3H_7)_{1.0}$	468	824	1.76
XIII	polymer **I** w/ethylene, 24 h, 25 °C	B 30.75, N, 42.39, H 6.73, C 19.56	$B_3N_{3.2}H_{2.4}(C_2H_5)_{0.9}$	1349	2887	2.14
	polymer **I** w/ethylene, 24 h, 25 °C	B 28.96, N 39.68, H 5.95, C 21.12	$B_3N_{3.17}H_{1.7}(C_2H_5)$	626	5344	8.54
XIV	polymer **I** w/propylene, 24 h, 25 °C	B 32.70, N 42.10, H 5.56, C 15.54	$B_3N_{3.0}H_{2.5}(C_3H_7)_{0.43}$	608	5046	8.30

[a] Molecular weights determined using LALLS. All others determined using viscometry.

μm. Ar^+ ion sputtering was performed using a differentially pumped ion gun operating at 3 kV with a beam current of 1 μA, yielding a spot size of 1 μm. X-ray powder diffraction (XRD) spectra were obtained on a Rigaku Geigerflex X-ray powder diffractometer.

Molecular Weight analysis. Molecular weight distribution averages were determined using size exclusion chromatography employing in-line viscometric detection (SEC/VISC). Chromatograms were obtained with a 150-CV SEC/VISC system (Millipore Co.) operated at 35 °C.

A bank of four Ultrastyragel SEC columns (Millipore Co.) with mean permeabilities 10^5, 10^4, 10^3, and 10^2 Å was employed. UV-grade THF (Burdick and Jackson Co.) was used as the mobile phase. A flow rate setting of 1.0 mL/min was employed. The actual flow rate was determined gravimetrically before the start of the analysis. An injection volume of 400 μL was used. Polymer solutions were prepared in a drybox to prevent hydrolysis. Concentrations of injected polymer solutions were typically 10 mg/mL.

A universal calibration curve was generated from the DRI chromatograms of sixteen nearly monodisperse ($M_w/M_n \leq 1.1$) polystyrene calibrants (Toya Soda Inc. and Polymer Laboratories Ltd.) ranging in molecular weight from 200 to 1.1×10^6 g/mol. The Mark–Houwink relationship needed for the universal calibration was obtained by using the SEC/VISC system to determine an intrinsic viscosity, $[\eta]$, for each calibrant. The resulting Mark–Houwink relationship for polystyrene in THF at 35 °C was

$$[\eta] = 1.2175 \times 10^{-4} M^{0.712} \quad (1)$$

where M is the peak molecular weight of the calibrant.

A third-order polynomial was least-squares fitted to the log hydrodynamic volume versus retention volume data. From this universal calibration curve, hydrodynamic volume at each chromatographic data point, ϕ_i, was determined. Intrinsic viscosity at the corresponding data point, $[\eta_i]$, was calculated from the combined outputs of the VISC and DRI detectors following previously described[21] methodology. Prior to these calculations, DRI and VISC chromatograms were offset to account for the time delay between the two detectors. Offset times were obtained from the peak elution times of chromatograms for the polystyrene calibrants. A delay time of 5.2 s was found. Concentrations at each chromatographic data point, c_i, were obtained from the DRI peak height, h_i, and the mass of polymer injected, m:

$$c_i = m(h_i)/(v_i)\sum h_i \quad (2)$$

where v_i is the incremental volume corresponding to data point i.

Molecular weight at each chromatographic point, M_i, was calculated from ϕ_i and $[\eta_i]$:

$$M_i = \phi_i/[\eta_i] \quad (3)$$

Molecular weight distribution averages, M_n, M_w, and M_z, were obtained by the appropriate summations of M_i and c_i across a chromatogram. Reported molecular weight averages are mean values of two determinations.

Data acquisition and reduction was provided by a micro pdp 11/23+ computer (Digital Equipment). Data acquisition was performed with a modified version of program MOLWT3 (Thermo Separations). Universal calibration and molecular weight calculations were performed with computer programs written to analyze MOLWT3-acquired SEC/VISC data.

SEC/LALLS molecular weight averages were determined by using the program MOLWT3 (Thermo Separations) with the DRI detector serving as the polymer mass detector. Prior to molecular weight calculations, the delay time between the detectors of the SEC/LALLS/UV system was determined by measuring the time differences between the LALLS, UV, and DRI chromatographic peak maxima for a 96 400 molecular weight polystyrene standard (M_w/M_n = 1.05). The raw responses from the DRI and UV detectors were offset by the measured delays (18.2 s for LALLS to DRI and 7.8 s for the LALLS to UV). In the case of UV chromatograms, there was no time delay for UV chromatograms obtained at different wavelengths (230 and 259 nm in the present study) since the UV detector monitored multiple wavelengths simultaneously. Molecular weight calculations performed by MOLWT3 have been previously described.[22]

Specific refractive index increments (dn/dc) for the polymers in THF at 25 °C were determined by using KMX-16 laser differential refractometer (Thermo Separations).

Polymer Synthesis. A summary of polymer syntheses and characterizations is found in Table 1.

Polymerization of Borazine. In a typical reaction, borazine (2.97 g, 36.9 mmol) was condensed at −196 °C into an evacuated Fischer-Porter glass pressure reaction vessel (part no. 100-205-0003) charged with a magnetic stirring bar. The flask was allowed to warm to room temperature and then heated at 70 °C. The reaction was allowed to continue, with periodic degassing, until the liquid became sufficiently viscous that stirring could not be continued (~48–60 h). The volatile materials were removed under high vacuum, leaving a white solid (2.27 g, 91% yield based on reacting borazine), **I**.

(21) Kuo, C.-Y.; Provder, T.; Koehler, M. E. *J. Liq. Chromatogr.* **1990**, *13*, 3177.

(22) Jordan, R. C. *J. Appl. Polym. Sci.* **1980**, *3*, 439.

Caution: *Heating gram quantities of borazine will produce large volumes of hydrogen. If polymerization is not done in a high-pressure vessel, frequent degassings are necessary.*

A sample of polymer (1.25 g) was dissolved in glyme and precipitated upon addition to pentane. Filtration and removal of residual solvent under dynamic vacuum yielded 0.839 g of fine, white polymer (67% yield), **II**.

I: IR (diffuse, KBr powder, cm^{-1}) 3445 (m), 3230 (br, m), 2505 (m), 1450 (br, s), 1200 (m), 900 (m), 750 (m), 690 (m). ^{11}B NMR (160.5 MHz, THF) 31 ppm (s, vbr). Density: 1.56 g/mL.

II: Spectroscopic data are consistent with that reported for **I**.

TGA studies of **I** indicate the polymer undergoes rapid decomposition in air. The polymer shows an early weight gain near 200 °C, continuing to around 450 °C. Between 450 and 800 °C little weight change occurs. Above 800 °C, a rapid increase occurs up to a total increase of about 20%, similar to that observed in boron nitride.

Fractionation of the volatile materials from the above reaction through −78 and −196 °C traps gave 23 mg of material stopping in the −78 °C trap. Recovered in the −196 °C trap was 0.480 g of borazine. GC/MS analysis showed the material stopping in the −78 °C trap was a mixture of borazanaphthalene and diborazine in a 1.7:1 ratio. Also observed in the ^{11}B NMR spectrum of the volatile component were small amounts (≤10%) of μ-aminodiborane,[23] which was not observed by GC/MS. Vacuum line fractionation of the reaction volatiles through a −30, −63, and −196 °C trap series allowed the separation of borazanaphthalene, $B_5N_5H_8$, in the −63 °C trap, and diborazine, 1:2′-$(B_3N_3H_5)_2$, in the −30 °C trap. In other reactions in which the volatile components were analyzed, borazanaphthalene and diborazine were produced in comparable yields and ratios.

1:2′-$(B_3N_3H_5)_2$: ^{11}B NMR (C_6D_6, 160.5 MHz, ppm) 29.7 (s, 1, $B_{2'}$), 31.2 (d, 1, B_4), 32.1 (d, 2, $B_{2,6}$ or $B_{4',6'}$) 32.5 (d, 2, $B_{4',6'}$ or $B_{2,6}$). $^1H\{^{11}B\}$ NMR (C_6D_6, 200 MHz, ppm) 4.39 (s, BH), 4.63 (s, BH), 4.99 (t, 45, NH), 5.08 (t, 54, NH), 5.34 (t, 42, NH). The infrared spectrum was consistent with that reported earlier.[10] Exact mass calcd for $^1H_{10}{}^{11}B_6{}^{14}N_6$, 159.1447, found 159.1442.

$B_5N_5H_8$: ^{11}B NMR (C_6D_6, 64 MHz, ppm) 35.5 (d, 137), 31.1 (d, 133), 25.8 (s). $^1H\{^{11}B\}$ NMR (C_6D_6, 200 MHz, ppm) 3.93 (t, br, NH), 4.48 (s, BH), 5.01 (s, BH), 5.01 (t, 50, NH). The infrared spectrum was consistent with that reported earlier.[11]

In other experiments, polyborazylene polymers were produced by heating samples of borazine at 70 °C for 48 h, **III**, 36 h, **IV** and 22 h, **V**, and the results of these syntheses are given in Table 1.

In a procedure similar to the above, borazine was heated at 110 °C for 9 h to give a soluble polymer, **VI**. The spectroscopic data for **VI** are consistent with that reported for **I**.

Solution Polymerization of Borazine. A solution of borazine in toluene, 69% w/w, was heated at 70 °C for 114 h. During the reaction period, polymer slowly precipitated from the solution to form a slurry. The slurry slowly thickened until the mixture no longer could be stirred. The volatiles were removed under reduced pressure and fractionated through −30 and −196 °C traps. Stopping in the −30 °C trap was 9 mg of material which was shown by GC/MS to be 2:1 ratio of borazanaphthalene and diborazine. Isolated from the reaction was 2.78 g (85% yield) of powdery polymer, **VII**.

VII: The infrared spectrum was consistent with **I**.

In another experiment, a solution of borazine in benzene, 33% w/w, was heated at 70 °C. During the reaction period the solution slowly became cloudy until it had a milky appearance. Volatile materials were distilled under reduced pressure and fractionated through a −30, −78, and −196 °C trap series. Stopping in the −30 °C trap was 130 mg of material which was shown by GC/MS to be borazanaphthalene and diborazine in a 1.7:1 ratio. The residue in the flask was a highly viscous material, **VIII**.

In a separate experiment, a solution of borazine in glyme, 9.4% w/w, was heated at 70 °C. At the end of the reaction period, the solution had become slightly cloudy. After removal of volatiles, a sticky solid remained in the flask, **IX**.

Polymerization of Diborazine. Diborazine (0.150 g, 0.9 mmol) was heated at 70 °C for 48 h. The volatile components were removed under vacuum and collected in a 196 °C trap. Isolated was 25 mg of material which was shown by GC/MS to be mostly diborazine, along with trace amounts of borazanaphthalene. The material retained in the flask was extracted with pentane. GC/MS showed it to be a mixture of borazanaphthalene (10%), diborazine (74%), a $B_7N_7H_{10}$ species (m/z = 185; 6%), and a $B_9N_9H_{14}$ species (m/z = 239; 10%) corresponding to a borazine trimer. Material not soluble in pentane was dissolved in glyme and analyzed by mass spectroscopy, showing masses above 400 amu.

Polymerization of *B*-Alkylborazines. *B*-Ethylborazine and *B*-propylborazine were produced by the $RhH(CO)(PPh_3)_3$-catalyzed borazine/olefin hydroboration reaction described elsewhere.[20] The *B*-ethylborazine (1.39 g) was polymerized by heating at 90 °C for 6 days at which point the solution no longer could be stirred, giving a transparent solid. The solid was dissolved in dry THF and was then precipitated by slowly adding the solution to pentane, **X**.

X: DRIFT (KBr powder, cm^{-1}) 3435 (m), 2950 (m), 2870 (m), 2510 (m), 1490 (vs, br), 895 (m), 765 (m), 695 (m).

In another experiment, a sample of *B*-ethylborazine was heated at 70 °C for 28 days, at which point the reaction mixture no longer could be stirred, giving a transparent solid, **XI**. The material was soluble in dry THF, chloroform, and benzene.

XI: IR (thin film, NaCl plates, cm^{-1}) 3420 (s), 2960 (s), 2940 (s, sh), 2920 (s), 2880 (s), 2520 (s), 1730 (w), 1460 (s, vbr), 1100 (w), 1020 (vw), 990 (vw), 900 (m), 760 (m), 690 (m).

In a separate experiment, a sample of *B*-propylborazine was heated at 70 °C for 28 days at which point the reaction mixture no longer could be stirred, giving a transparent solid, **XII**. The material was soluble in dry THF, chloroform, and benzene.

XII: IR (thin film, NaCl plates, cm^{-1}) 3440 (s), 2980 (s), 2930 (s), 2910 (s), 2880 (s), 2810 (m, sh), 2750 (w), 2520 (m), 1440 (s, vbr), 1200 (s), 1135 (s), 1100 (s), 1070 (m), 1025 (m), 990 (vw), 900 (s), 840 (m), 825 (m), 735 (s), 700 (s).

Alkylation of Polyborazylene. *B*-Ethylpolyborazylene and *B*-propylpolyborazylene were prepared by the reaction of polyborazylene with ethylene or propylene in glyme solution in the presence of catalytic amounts of $RhH(CO)(PPh_3)_3$, as described previously,[20] to give polymers of composition $B_3N_{3.2}H_{2.4}(C_2H_5)_{0.9}$ (**XIII**, density 1.4 g/mL) and $B_3N_{3.0}H_{2.5}(C_3H_7)_{0.43}$ (**XIV**), respectively.

Ceramic Conversion Reactions. Crude and precipitated polymer samples (~1.0−1.5 g) were pyrolyzed in boron nitride boats under flowing argon or ammonia with a ramp rate of 5 °C/min until the furnace reached the set temperature. The furnace was held at this temperature for 12 h and then allowed to cool slowly to room temperature.

The argon (99.999%) was purchased from Airco and MG and was further purified by passing through an oxygen scavenger (Lab Clear, O_2 < 1 ppm) that was installed between the gas tank and the tube furnace. Ammonia (electronic grade) was purchased from Matheson and used as received. Boron nitride pyrolysis boats were carved from boron nitride obtained from Union Carbide. Quartz tubes were used for pyrolyses at 900 °C or below. Mullite furnace tubes obtained from Vesuvius McDanel (part no. MV30) were used for pyrolysis above 1000 °C. Pyrolyses were performed in a Lindberg 58000 series tube furnace with an Eurotherm 818 temperature control unit.

The results of pyrolysis experiments are summarized in Table 2. The resulting materials were white in appearance and characterized by elemental analysis, powder XRD, DRIFT spectra, density, and their resistance to oxidation as summarized in Table 3.

In a separate experiment, polyborazylene (1.626 g) was heated under argon flow at a rate of 5 °C/min until the furnace temperature reached a maximum temperature of 400 °C. The furnace was held at this temperature for 2 h and then slowly cooled to room temperature. The resulting material was a white powder (1.530 g, 94% ceramic yield) that was insoluble in THF, DMF, and DMSO. DRIFT (KBr, cm^{-1}) 3455 (m), 2505

(23) Gaines, D. F.; Schaeffer, R. *J. Am. Chem. Soc.* **1964**, *86*, 1505−1507.

Table 2. Pyrolysis Reaction Summary

expt[a]	temp, atmosphere[c]	polym wt, g	ceramic wt, g	ceramic yield, %	chemical yield,[d] %
A[b]	900 °C, Ar	1.507	1.360	90	95
B	1200 °C, Ar	1.148	0.982	86	90
C	1500 °C, Ar	1.243	1.049	84	89
D	900 °C, NH_3	1.026	0.956	93	99
E	1200 °C, NH_3	1.089	0.957	88	93
F	1450 °C, NH_3	1.100	0.959	87	92

[a] All polymers used were obtained by heating borazine at 70 °C for at least 48 h. [b] Experiments A, B, and C used crude polymer samples. Experiments D, E, and F used precipitated polymers. [c] All pyrolyses were done for 12 h. [d] Based upon an ideal polymer of $B_3N_3H_4$ (FW = 78.84) and the reaction $(B_3N_3H_4)_x \rightarrow 3BN + 2H_2$.

Table 3. Ceramic Characterization

experiment	elem anal.	B to N ratio	$d(002)$, Å	density, g/mL
A	B 42.47; N, 52.90; H, <0.5; C, <0.5	$B_{1.04}N_{1.0}$	3.54	1.78
B	B, 40.00; N, 54.79; H, <0.5; C, <0.5	$B_{1.0}N_{1.06}$	3.58	1.72
C	B, 43.03; N, 56.44; H, <0.5; C, <0.5	$B_{1.0}N_{1.01}$	3.39	1.92
D	B, 38.88; N, 51.81; H, 0.63; C, 0.54	$B_{1.0}N_{1.03}$	3.63	1.76
E	B, 42.08; N, 54.52; H, <0.5; C, <0.5	$B_{1.0}N_{1.0}$	3.55	1.81
F	B, 40.50; N, 53.25; H, <0.5; C, <0.5	$B_{1.0}N_{1.02}$	3.43	2.04

(m), 1460 (vs, vbr) 910 (m), 760 (m), 690 (m). Anal. Found: B 40.35; N 53.76; H 2.32; C <0.5%. Density 1.75 g/mL

Alkyl polymer **XII** (0.224 g) was pyrolyzed at 1000 °C for 12 h to give 0.188 g (80% ceramic yield) of a ceramic which gave a microanalysis of B 31.11, N 37.66, C 2.00, H 1.25 and a measured density of 1.75 g/mL. Two other polymer samples (with analyses of B 36.32, N 47.78, C 6.23, H 4.84% (0.282 g) and B 36.27, N 46.91, C 5.31, H 4.78% (0.236 g)) gave upon pyrolysis to 1000 °C under argon, gray ceramic materials with analyses of B 35.49, N 46.97, C 1.54, H 1.37% (0.244 g, 86% ceramic yield, density 1.87 g/mL) and B 34.33, N 47.43, C 1.70, H 1.47% (0.199 g, 84% ceramic yield, density 1.92 g/mL), respectively. Polymers **XI** (0.146 g) and **XII** (0.164 g) were pyrolyzed at 1000 °C for 12 h under argon flow. The resulting ceramics (0.050 g, 34% ceramic yield; 0.052 g, 31% ceramic yield) had analyses of B 29.38, N 34.93, C 4.95, H 2.07% and B 31.44, N 39.74, C 6.37, H 1.23%, respectively. DRIFT and XRD spectra of the ceramics indicate the presence of turbostratic boron nitride.

Fiber Coatings. Solutions used for fiber coatings were prepared by dissolving crude polyborazylene in glyme. Carbon fibers (P-55) were obtained from Dr. James Sheehan of MSNW Co. DuPont PRD-166 (Al_2O_3/ZrO_2) fibers were obtained from Dr. John Bolt of DuPont Central Research and Development and were pretreated by heating to 600 °C in air. Fiber bundles were "hand dipped" under argon using forceps. After solvent evaporation the fiber bundles were somewhat stiff. At this point they were then placed in a boron nitride boat that was transferred to a tube furnace. The pyrolysis tube was purged with ammonia or argon for several minutes and then the temperature was increased at a rate of 10 °C/min to a maximum temperature of 1000 °C. The temperature was held for 12 h and then allowed to cool to room temperature. The resulting boron nitride coated fibers were flexible. When more concentrated solutions (>8% w/w) were used, the fibers appeared fused together. Coatings were characterized by AES.

Collection and Refinement of the Data. X-ray intensity data for diborazine were collected on an MSC/AFC7R diffractometer employing graphite-monochromated Cu Kα radiation (λ = 1.541 84 Å) at 193 K using the $\omega-2\theta$ scan technique. X-ray data were processed, and the structure was solved and refined using the Molecular Structure Corp. teXsan[24] package on a Silicon Graphics Indigo R4000 computer. X-ray intensity data for borazanaphthalene were collected on an Enraf-Nonius CAD4 diffractometer employing graphite-monochromated Mo Kα radiation (λ = 0.710 73 Å) at 213 K and using the $\omega-2\theta$ scan technique. X-ray data were processed, and the structure was solved and refined using the Enraf-Nonius MolEN[25] package on a DEC MicroVAX 3100 computer.

Table 4. Data Collection and Structure Refinement Information

compound	1:2′-diborazine	borazanaphthalene
formula	$B_6H_{10}N_6$	$B_5H_8N_5$
formula wt	158.98	132.15
crystal class	monoclinic	orthorhombic
space group	$C2/c$ (No. 15)	$Pna2_1$ (No. 33)
Z	4	8
cell constants		
a, Å	9.320(2)	12.426(2)
b, Å	20.255(2)	5.184(5)
c, Å	5.462(2)	22.386(6)
β, deg	121.57(1)	
V, Å^3	878.6(4)	1442(2)
μ, cm^{-1}	5.89	0.71
crystal size, mm	0.55 × 0.35 × 0.25	0.32 × 0.16 × 0.08
D_{calc}, g/cm^3	1.202	1.217
radiation	Cu Kα (λ = 1.541 84 Å)	Mo Kα (λ = 0.710 73 Å)
θ range	2.0−60.0	2.0−27.5
scan mode	$\omega-2\theta$	$\omega-2\theta$
h, h, l collected	+10, +22, ±6	+6, +16, +29
no. reflns measured	682	1962
no. unique reflns	648	1688
no. reflns used in refinement ($F^2 > 3.0\sigma$)	477	860
no. parameters	77	180
data parameter ratio	6.20	4.8
R_1	0.080	0.060
R_2	0.092	0.067

Table 5. Refined Positional Parameters for 1:2′-$(B_3N_3H_5)_2$[a]

atom	x	y	z	B_{eq}, Å^2
N1	1/2	0.2192(2)	3/4	3.0(2)
N1′	0.4162(4)	0.3300(2)	0.8579(8)	3.7(1)
N3	0.5799(4)	0.1128(2)	0.6359(8)	4.1(1)
N4′	1/2	0.4334(2)	3/4	4.0(2)
B2	0.5847(5)	0.1819(2)	0.638(1)	3.7(2)
B2′	1/2	0.2915(3)	3/4	3.0(2)
B3′	0.4126(6)	0.3990(2)	0.860(1)	4.1(2)
B4	1/2	0.0757(3)	3/4	4.2(3)
H1′	0.388(6)	0.311(2)	0.96(1)	5(1)
H2	0.642(5)	0.208(2)	0.53(1)	5(1)
H3′	0.355(4)	0.428(2)	0.956(8)	4.6(8)
H3	0.611(6)	0.091(2)	0.53(1)	6(1)
H4	1/2	0.018(3)	3/4	7(2)
H4′	1/2	0.477(3)	3/4	4(1)

[a] Hydrogen atoms were refined isotropically. $B_{eq} = 8/3[U_{11}(aa^*)^2 + U_{22}(bb^*)^2 + U_{33}(cc^*)^2 + 2U_{12}aa^*bb^* \cos\gamma + 2U_{13}aa^*cc^* \cos\beta + 2U_{23}bb^*cc^* \cos\alpha]$.

Solution and Refinement of the Structure. The structures of diborazine and borazanaphthalene were solved by direct methods (MULTAN11/82 and SIR88). Refinement was by full-matrix least-squares techniques based on F to minimize the quantity $\sum w(|F_o| - |F_c|)^2$ with $w = 1/\sigma^2(F)$. Non-hydrogen atoms were refined anisotropically and hydrogen atoms were included as constant contributions to the structure factors and were not refined. Refinement for diborazine converged to R_1 = 0.080 and R_2 = 0.092 and for borazanaphthalene converged to R_1 = 0.060 and R_2 = 0.067.

Table 4 lists cell information, data collection parameters, and refinement data. Final positional and equivalent isotropic thermal parameters for diborazine are given in Table 5 and for borazanaphthalene in Table 6. Tables 7 and 8 list refined bond distances for diborazine and borazanaphthalene, respectively.

(24) teXsan: Crystal Structure Analysis Package, Molecular Structure Corp. 1985, 1992.

(25) MolEn, An Interactive Structure Solution Procedure, Enraf-Nonius: Delft, The Netherlands, 1990.

Table 6. Refined Positional Parameters for $B_5N_5H_8$[a]

atom	x	y	z	B_{eq}, Å^2
N1	0.0402(3)	−0.1773(9)	0.161	3.68(9)
N3	0.1196(3)	−0.337(1)	0.0712(2)	4.3(1)
N6	−0.1471(3)	0.3632(9)	0.0633(2)	4.6(1)
N8	−0.0935(3)	0.1848(9)	0.1580(2)	3.59(9)
N10	−0.0125(3)	0.0142(8)	0.0653(2)	3.26(9)
B2	0.1119(5)	−0.352(2)	0.1349(3)	4.7(2)
B4	0.0601(5)	−0.159(1)	0.0355(3)	4.4(2)
B5	−0.0738(5)	0.202(1)	0.0320(3)	4.7(2)
B7	−0.1568(5)	0.368(1)	0.1266(3)	4.4(2)
B9	−0.0213(5)	0.008(1)	0.1300(3)	3.9(1)
N1′	0.3069(3)	−0.189(1)	0.2815(2)	4.1(1)
N3′	0.3797(3)	−0.3240(9)	0.3766(2)	4.1(1)
N6′	0.1139(3)	0.3687(9)	0.3716(2)	5.1(1)
N8′	0.1712(3)	0.173(1)	0.2785(2)	4.2(1)
N10′	0.2479(3)	0.0246(8)	0.3749(2)	3.50(9)
B2′	0.3756(5)	−0.356(1)	0.3130(3)	3.9(1)
B4′	0.3161(5)	−0.143(1)	0.4076(3)	3.6(1)
B5′	0.1834(5)	0.215(1)	0.4056(3)	3.9(1)
B7′	0.1056(5)	0.358(1)	0.3082(3)	4.8(2)
B9′	0.2404(4)	0.004(1)	0.3102(3)	3.1(1)

[a] $B_{eq} = {}^4/_3[\beta_{11}a^2 + \beta_{22}b^2 + \beta_{33}c^2 + \beta_{12}ab\cos\gamma + \beta_{13}ac\cos\beta + \beta_{23}bc\cos\alpha]$.

Table 7. Selected Bond Distances (Å) for 1:2′-$(B_3N_3H_5)_2$

N1−B2	1.439(5)	N1−B2′	1.464(7)
N1′−B2′	1.430(4)	N1′−B3′	1.399(5)
N1′−H1′	0.807(42)	N3−B2	1.401(6)
N3−B4	1.412(5)	N3−H3	0.869(45)
N4′−B3′	1.421(5)	N4′−H4′	0.892(54)
B2−H2	1.111(40)	B3′−H3′	1.105(37)
B4−H4	1.160(61)		

Table 8. Selected Bond Distances (Å) for $B_5N_5H_8$

N1−B2	1.400(8)	N10−B4	1.438(8)
N6′−B7′	1.424(9)	N1−B9	1.409(8)
N10−B5	1.445(8)	N8′−B7′	1.420(8)
N3−B2	1.432(8)	N10−B9	1.453(8)
N8′−B9′	1.420(7)	N3−B4	1.426(8)
N1′−B2′	1.404(8)	N10′−B4′	1.418(7)
N6−B5	1.419(8)	N1′−B9′	1.449(7)
N10′−B5′	1.444(8)	N6−B7	1.423(7)
N3′−B2′	1.434(8)	N10′−B9′	1.455(7)
N8−B7	1.419(8)	N3′−B4′	1.409(7)
N8−B9	1.427(8)	N6′−B5′	1.400(8)

Results and Discussion

Polyborazylene Synthesis. Borazine was found to readily dehydropolymerize in the liquid state when heated in vacuo at 70 °C for 48−60 h. It was observed that as the reaction proceeded the reaction mixture became highly viscous and the heating was stopped when the mixture was too thick to stir. At that point, the reaction vessel was degassed at −196 °C to remove the evolved hydrogen. The mixture was allowed to warm to room temperature, and any volatile components were vacuum evaporated into the vacuum line. Remaining in the flask was a moisture-sensitive white solid. The solid could be handled quickly in air, crumbled easily, and was soluble in ethers such as glyme and THF. Yields for the crude polymer prepared in this way ranged from 81 to 91% for the reactions in Table 1. The crude polymer could then be precipitated by dropping the THF solution into pentane.

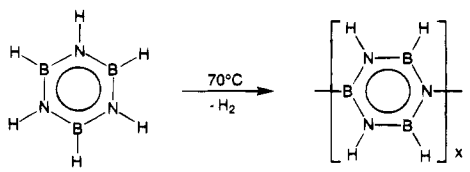

(4)

Although the polymer may be handled for short periods in air without significant decomposition, TGA studies indicate that it readily decomposes in air at higher temperatures (≲200 °C). Likewise, the polymer undergoes rapid hydrolysis in solution and should therefore be handled only in anhydrous solvents.

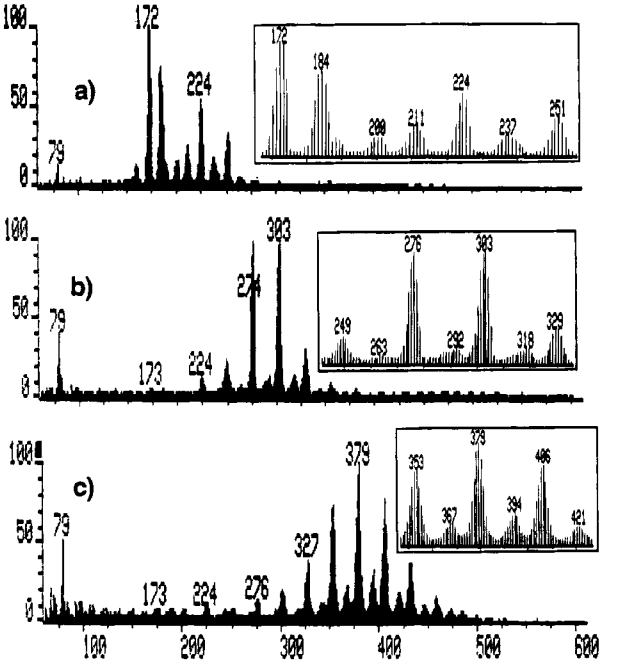

Figure 1. Mass spectra of polyborazylene heated to successively higher temperatures [(a) → (b) → (c)] with expanded views to the right.

As illustrated in Table 1, elemental analyses of these polymers gave a range of empirical formulas from $B_3N_3H_{3.4}$ to $B_3N_3H_{3.9}$ for crude polymers and from $B_3N_3H_{2.65}$ to $B_3N_3H_{3.8}$ for precipitated samples. The average formula for the crude polymers was $B_3N_{3.1}H_{3.6}$, while that of the precipitated polymers was $B_3N_{3.1}H_{3.4}$. A simple polyborazylene polymer that would result from a borazine dehydrocoupling process would have a formula of $\sim B_3N_3H_4$; therefore, the somewhat lower hydrogen ratio suggests a partially cross-linked structure, or a structure containing some fused or polycyclic ring systems. These conclusions are likewise supported by the molecular weight studies discussed later.

The spectroscopic data are consistent with the presence of borazine rings in the polymer. The DRIFT spectrum shows the B−N stretch near 1460 cm^{-1} and the B−N−B bending mode at ~900 cm^{-1}, characteristic of the borazine ring.[26] Also present are absorptions near 3450 and 2500 cm^{-1} due to ring N−H and B−H stretches. Likewise, its ^{11}B NMR spectrum shows a very broad featureless resonance centered around 30 ppm, which is in the chemical shift range normally observed for borazine ring compounds.[27]

Mass spectral studies of the precipitated polymer, in which the polymer was heated on a probe under chemical ionization conditions, show masses above 500 amu (Figure 1). The envelope at 394 amu would correspond to a $(B_3N_3H_4)_5$ unit and a comparison of the isotope distribution for a B_{15} fragment is in reasonable agreement with the observed pattern. Molecular weight studies, discussed later, indicate much higher molecular weights, but to observe higher masses by mass spectrometry, other techniques, such as field desorption,

(26) *Gmelin Handbush der Anorganishen Chemie, Borazine and Its Derivatives*; Springer-Verlag: New York, 1978; Vol. 17.

(27) Nöth, H.; Wrackmeyer, B. *Nuclear Magnetic Resonance Spectroscopy of Boron Compounds*; Springer-Verlag: New York, 1978; pp 48−51.

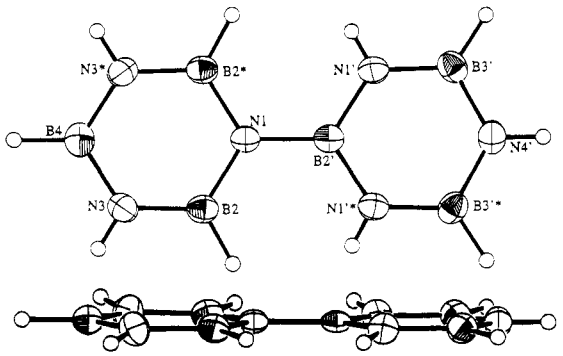

Figure 2. ORTEP views of the molecular structure of diborazine, 1,2′-$(B_3N_3H_5)_2$.

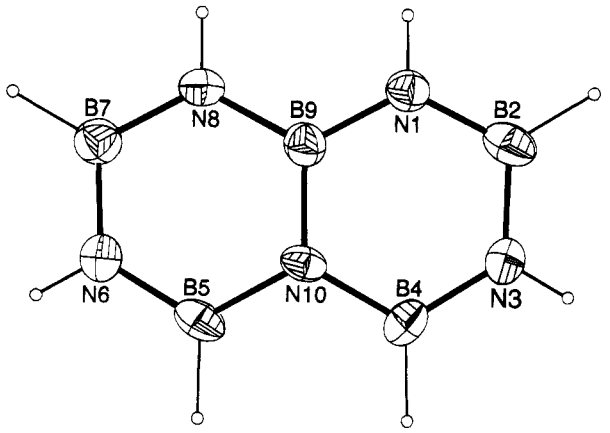

Figure 3. ORTEP drawing of molecular structure of borazanaphthalene, $B_5N_5H_8$.

would be required. Fragment peaks show a pattern of separation of 27 amu, consistent with loss of a BNH_2 unit. Loss of this fragment has been reported in earlier mass spectral studies of borazine species.[14]

Although the detailed structure of the polymer may well be complex, the N:B coupled dimer, 1:2′-$(B_3N_3H_5)_2$, and borazanaphthalene, $B_5N_5H_8$, provide models for the major polymer structural units. Both compounds were observed as volatile side products in low yields (~1–3%) and in an ~2:1 borazanaphthalene-to-diborazine ratio in all polymerization reactions. Kim and Economy[28] have likewise observed by mass spectrometry the formation of these two compounds when they have carried out this polymerization. As mentioned in the Introduction, diborazine and borazanaphthalene were originally isolated by Laubengayer,[11,12] but neither their X-ray structural determinations nor their NMR spectra have previously been reported. The compounds were separated by vacuum-line fractionation into −30 and −63 °C traps and isolated as crystalline solids. The crystals were then sublimed into detachable U-traps and transferred to capillaries in glovebags. The capillaries were then mounted on the diffractometer and the X-ray determinations carried out at low temperatures. ORTEP drawings of the molecular structures of diborazine and borazanaphthalene are shown in Figures 2 and 3, respectively. The determinations confirm the previously proposed structures, with diborazine having a linked ring structure analogous to that of biphenyl and borazanaphthalene having a fused-ring structure similar to that of naphthalene.

The structure of diborazine confirms the existence of a B–N bond connecting the two borazine rings. The intraring B–N bonds are between 1.399(5) and 1.439(5) Å, and are in the ranges of the intraring B–N bonds found in borazine (1.429(1) Å)[29] and the bisborazinylamines.[30] These distances are shorter than normal B–N single-bonds (~1.58 Å) and in the range observed for B–N double-bond distances (~1.41 Å).[31] They are also slightly longer than the intraring bonds in biphenyl (1.379(3)–1.399(3) Å).[32] The inter-ring bond in diborazine (1.464(7) Å) is slightly longer than the intraring distances but shorter than the inter-ring distance found in biphenyl (1.493(3) Å). Unlike in the bisborazinylamines where the two borazinyl rings are significantly twisted with respect to each other,[30] the two borazine rings in diborazine are coplanar, as in biphenyl, again suggesting the short inter-ring bond results from multiple-bond character. It should be noted that recent ab initio calculations[33] indicate that although the lowest energy structure of diborazine has a dihedral angle of ~20° between the planes of the rings, the planar conformation is only about 0.13 kcal/mol higher in energy; and, as in biphenyl, the orientation with the rings perpendicular is substantially higher in energy. In the X-ray determined structure, the ortho hydrogens of diborazine, H1′ and H2*, are 2.122(57) Å apart, which is somewhat longer than the distance between the ortho hydrogens of biphenyl, 2.056 Å.[34] The greater distance between the hydrogens in diborazine may allow less steric interaction compared to biphenyl. Consistent with the X-ray structure determination, the ^{11}B NMR spectrum of diborazine (Figure 4a) shows four resonances: two intensity-two doublets, and a doublet and singlet each of intensity one. All four resonances occur in the chemical shift range of the broad resonance observed in the ^{11}B NMR spectrum of the polyborazylene polymer.

The isolation and structural determination of diborazine from the polymerization volatiles provides further evidence that the dehydropolymerization reaction proceeds via the formation of B–N linked borazine rings in the polymer. Consistent with this conclusion it was found that when pure samples of diborazine were heated at 70 °C for 48 h, oligomeric species were produced.

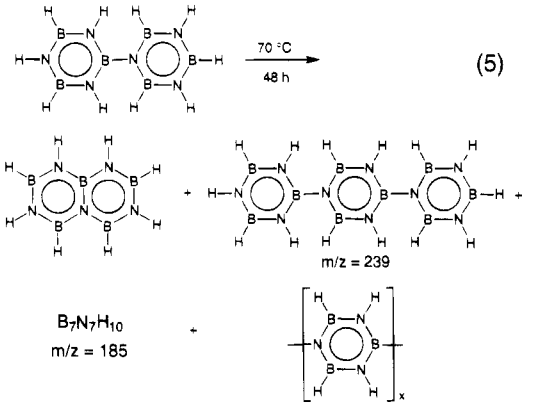

The product mixture was a viscous liquid (diborazine is a solid at room temperature). GC/MS analysis of the

(28) Kim, D.-P.; Economy, J. *Chem. Mater.* **1994**, *6*, 395–400.

(29) Boese, R.; Maulitz, A. H.; Stellberg, P. *Chem. Ber.* **1994**, *127*, 1887–1889.

(30) Narula, C. K.; Lindquist, D. A.; Fan, M.-M.; Borek, T. T.; Duesler, E. N.; Datye, A. K.; Schaeffer, R.; Paine, R. T. *Chem. Mater.* **1990**, *2*, 377–384.

(31) Paetzold, P. *Adv. Inorg Chem.* **1987**, *31*, 123–170 and references therein.

(32) (a) Charbonneau, G.-P.; Delugeard, Y. *Acta Crystallogr.* **1976**, *B32*, 1420–1423. (b) Charbonneau, G.-P.; Delugeard, Y. *Acta Crystallogr.* **1977**, *B33*, 1586–1588.

(33) Wille, A. E.; Sneddon, L. G. Unpublished results.

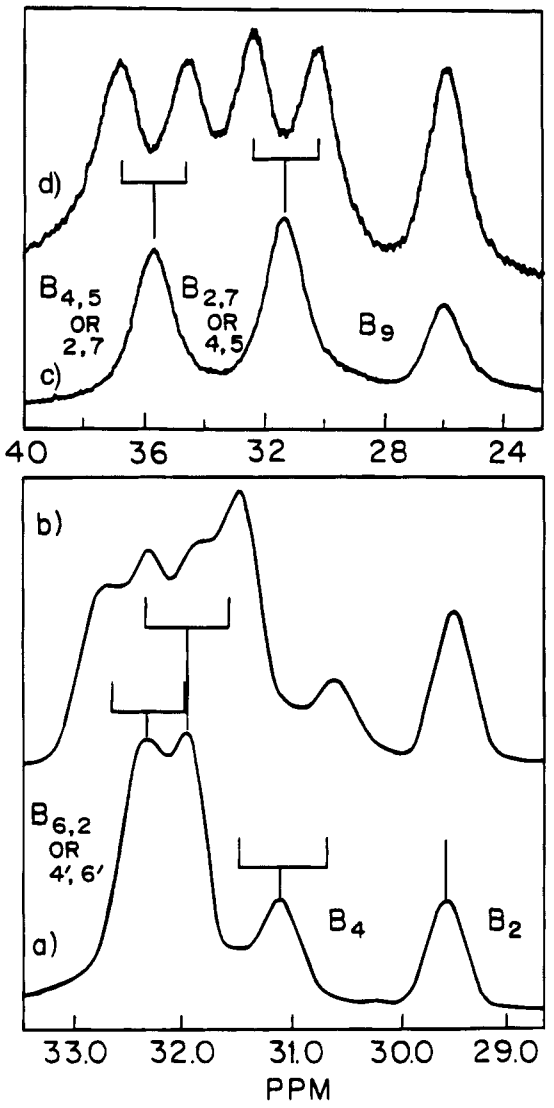

Figure 4. ^{11}B NMR spectra of diborazine (a) ^1H decoupled, (b) ^1H coupled, and borazanaphthalene (c) ^1H decoupled, (d) ^1H coupled.

lower-volatile pentane-soluble reaction products showed, in addition to unreacted diborazine and small amounts of borazanaphthalene, one species with m/z = 185, displaying a seven-boron pattern which would correspond to an anthracene type ring system, $B_7N_7H_{10}$, and another with m/z = 239, corresponding to a borazine trimer, $B_9N_9H_{14}$. Laubengayer[11,12] had also previously noted the formation of species with m/z = 185 in his studies of borazine pyrolysis. The mass spectra of the glyme soluble products showed (Figure 5) masses up to 488 amu along with strong patterns for borazine dimers and trimers.

The X-ray determined structure of borazanaphthalene (Figure 3) exhibits a fused-ring structure similar to that of naphthalene and is consistent with that proposed by Laubengayer. The B–N distances, ranging from 1.400(8) to 1.453(8) Å, fall within the range expected for a borazine species, again suggesting multiple bond character, and are somewhat longer than those found for C–C bond distances in naphthalene, which range from 1.378(2) to 1.426(2) Å.[35] The ^{11}B NMR spectrum (Figure 4b) which shows two doublets and a singlet, is again in

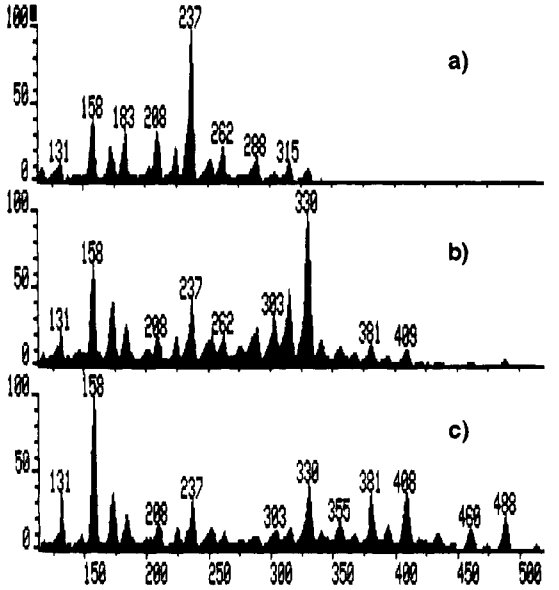

Figure 5. Mass spectra of the diborazine derived polymer heated to successively higher temperatures [(a) → (b) → (c)].

the range expected for borazine ring compounds. The presence of some fused polycyclic structural units in the polyborazylene polymer similar to that found in borazanaphthalene would be consistent with the lower hydrogen content of the polymer. Such condensed polycyclic fragments could easily arise from interchain and intrachain dehydrocoupling reactions. For example, an ortho-substituted trimeric segment could undergo dehydrocoupling between the 1 and the 3 rings and form a fused ring segment, as depicted here:

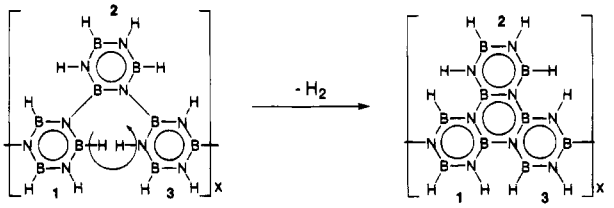

In addition to diborazine and borazanaphthalene, small amounts of μ-aminodiborane, $B_2H_5NH_2$, were also isolated from the volatile products of several of the borazine polymerization reactions. This compound could arise from a cleavage reaction of a borazine ring and such a process could, of course, also yield more complex condensed-fragments in the polymer.

Borazine polymerization reactions were also explored in benzene or toluene solution. When borazine was polymerized in toluene solution, 69% w/w, over a period of 5 days, polymer slowly precipitated from solution, forming a slurry. At the end of the reaction period the reaction mixture was too viscous to stir. After vacuum evaporation of solvent and reaction volatiles, a fine powder, which resembled those of precipitated polyborazylene, was isolated with M_n = 849 (see Table 1). A similar reaction with a lower concentration (33% w/w) of borazine gave a lower molecular weight material with M_n = 300. In another reaction, a 9.4% w/w solution of borazine in glyme was heated at 70 °C for 9 days. At the end of this period, the solution had become cloudy. Molecular weight studies indicate a very highly chain-branched material, as discussed below, with M_n = 561.

Molecular Weight Analysis. Polymer molecular weight distributions averages were determined by SEC/

(34) Tsuzuki, S.; Tanabe, K. *J. Phys. Chem.* **1991**, *95*, 139–144.
(35) Brock, C. P.; Dunitz, J. D. *Acta Crystallogr.* **1982**, *B38*, 2218–2228.

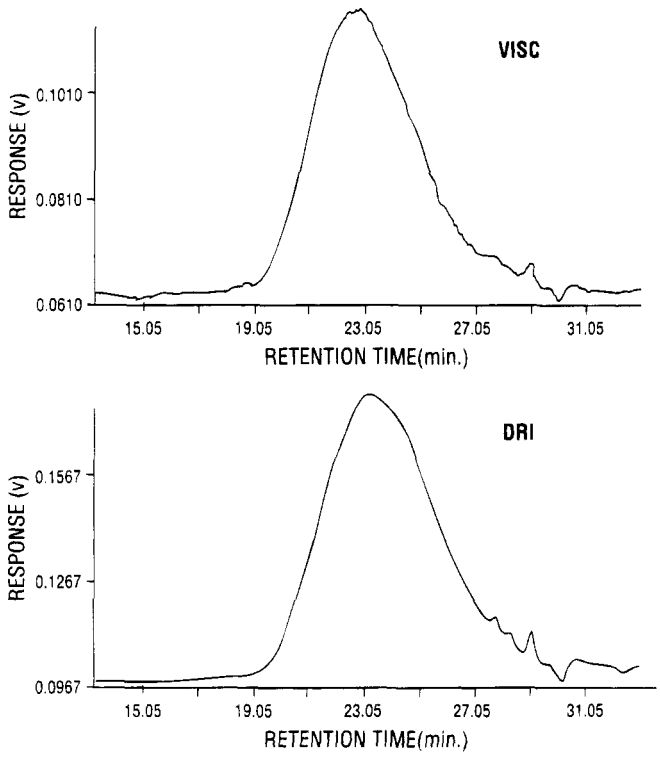

Figure 6. SEV/VISC chromatograms of polyborazylene.

LALLS/UV and SEC/VISC. The accuracy and reproducibility of molecular weight analysis via SEC/LALLS/UV were diminished by low signal/noise (S/N) in the low-angle laser light scattering (LALLS) detector's chromatogram of polymers with M_w less than 3000 g/mol.

The viscometric (VISC) detector used in the SEC/VISC analysis was more sensitive than the LALLS detector to low molecular weight polymers. Viscosity chromatograms had higher S/N than LALLS chromatograms, resulting in more accurate and reproducible molecular weight determinations. Representative SEC/VISC chromatograms for polyborazylene are shown in Figure 6.

Molecular weight distribution averages calculated from SEC/VISC and SEC/LALLS/UV data for polyborazylenes and alkylated polyborazylenes are summarized in Table 1. In general, SEC/LALLS/UV molecular weight averages were higher than those determined by SEC/VISC for polymers prepared under the same conditions (see Table 1). This apparent discrepancy is attributable to differences in response characteristics of the LALLS and VISC detectors. The LALLS detector is well-known[36] to have enhanced sensitivity in the high molecular weight region of a size-exclusion chromatogram. Strong response to a high molecular weight fraction will result in a M_w biased toward high molecular weight. The SEC/LALLS data shown in Figure 7 illustrate the skewing of LALLS detector response for a representative polyborazylene containing a high molecular weight component. The data in Figure 7 also show the characteristic, reduced response of the LALLS detector in the low molecular weight region of the chromatogram. This results in overestimation of M_n because lower molecular chains are not included in the calculation of distribution averages.

(36) Su, K.; Remsen, E. E.; Thompson, H.; Sneddon, L. G. *Macromolecules* **1991**, *24*, 3760–3766.

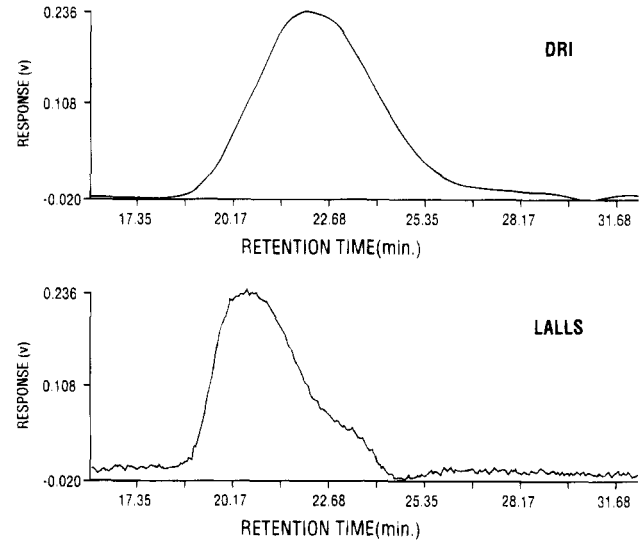

Figure 7. DRI/LALLS chromatograms of polyborazylene.

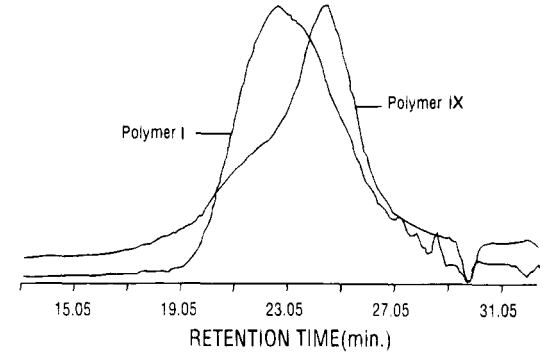

Figure 8. DRI chromatograms of Polymer **IX** and Polymer **I**.

In contrast to the LALLS, the VISC detector has greater sensitivity for low molecular weight fractions and the resulting lower value of M_n (compared to the LALLS-derived value) more accurately evaluate the true M_n of the polymer.

The high molecular weight fraction noted in some polyborazylene LALLS chromatograms suggested the presence of microgels or branched polymer. Additional evidence for branching was found in comparative intrinsic viscosity–molecular weight data obtained by SEC/VISC for polymers prepared under different conditions. As shown in the overlaid DRI chromatograms in Figure 8, solution polymerization of borazine produced a polymer (polymer **IX**, in Table 1) with significantly larger high molecular weight fraction than is observed in a liquid polymerized polymer (typical for polymer **I**, in Table 1). The molecular weight distribution averages for polymer **IX** (M_w =16 700 g/mol and M_z = 382 400 g/mol), reflect its high molecular weight component relative to the values measured for a sample of polymer **I** (M_w = 6500 g/mol and M_z = 30 100 g/mol). However, the calculated weight-average intrinsic viscosity ($[\eta]_w$) for the polymer was nearly identical: $[\eta]_w$ (polymer **IX**) = 0.41 dL/g; $[\eta]_w$ (polymer **I**) = 0.42 dL/g. The near equivalence of $[\eta]_w$ for compositionally identical polymers with different average molecular weight indicates that polymer **IX** has a smaller average hydrodynamic volume due to chain branching.

The presence of chain branching in higher molecular weight polyborazylenes is also suggested by the overlaid UV (230 nm) and DRI detector chromatograms shown in Figure 9. Detector lag time-corrected DRI and UV

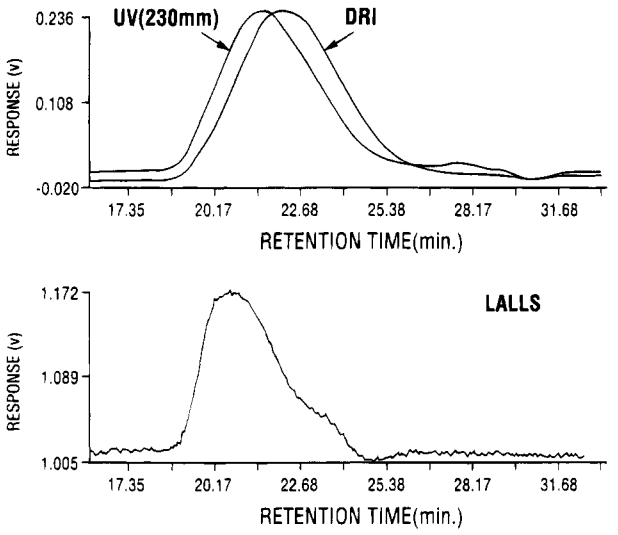

Figure 9. (a) UV/DRI and (b) LALLS chromatograms of polyborazylene.

chromatograms in Figure 9 are clearly offset. The UV chromatogram peaks at an earlier time than the DRI chromatogram. If the molar absorptivity of the polymer is assumed to be invariant with chain length, the increased UV absorption at early elution time relative to the DRI chromatogram, indicates the presence of more UV-absorbing groups (borazines) in earlier eluting fractions. This suggests more borazines per unit hydrodynamic volume in the earlier eluting fractions than in late-eluting fractions. Branched chains in early-eluting fractions would account for higher borazine content in this chromatographic region.

This interpretation is consistent with intrinsic viscosity–molecular weight results and elemental composition data discussed above. However, the validity of the underlying assumption—invariance of molar absorptivity with chain length—has not been established. The reliability of this assumption is uncertain based on previous studies of the analogous polymer, *p*-polyphenylene,[6a] which indicate that *p*-polyphenylene's UV absorption spectrum red-shifts and increases in molar absorptivity with increasing condensation of phenylene units. Consequently, further study is needed to determine if the correlation between the intensity of polyborazylene UV absorbance and chain branching is coincidental.

Alkyl-Substituted Polyborazylenes. As will be shown in a later section, polyborazylene is an excellent polymeric precursor to boron nitride that can be used for a number of applications. However, one drawback to the parent polymer is that it is not meltable, since it cross-links before melting. This cross-linking reaction results from a dehydrocoupling process that produces B–N bonds between different polymer chains. One approach to altering the properties of the polymer would be to inhibit the cross-linking reaction by substituting the reactive B–H or N–H hydrogens on the polymer with a substituent such as an alkyl. Such a substituent could also have the added advantage of increasing the solubility of the polyborazylene polymer.

It was found that *B*-alkyl-substituted polyborazylenes can be synthesized by two different methods. The first involved thermal polymerization of *B*-alkylborazines, as shown in eq 6. The needed monoalkylborazines were readily obtained by transition-metal catalyzed borazine/olefin hydroboration reactions as outlined in eq 7.[20]

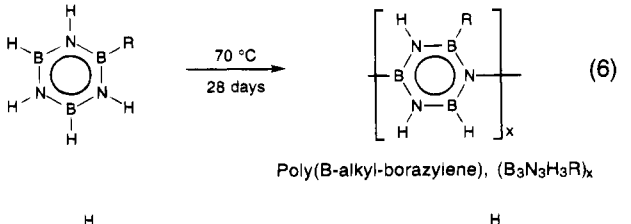

(6)

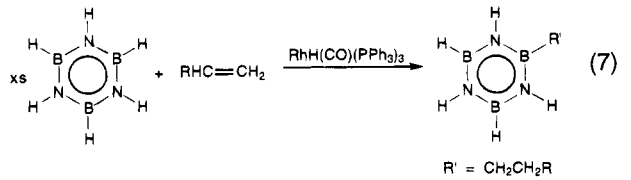

(7)

The thermal polymerization of *B*-alkylborazines required longer times than the parent compound. Samples of *B*-ethyl- and *B*-propylborazine were heated at 70 °C for weeks without showing the change in viscosity or the hydrogen evolution that occurs with borazine within 48 h. Only after a month did they become viscous enough to inhibit stirring.

These polymers were characterized by their elemental analysis, IR, and DRIFT spectra, mass spectroscopy, and by ^1H and ^{11}B NMR. Infrared spectra of all alkylborazine polymers show the presence of alkyl C–H stretches (2810–2980 cm^{-1}) and a decrease of the B–H stretches (2510–2520 cm^{-1}) relative to the N–H (3420–3440 cm^{-1}) stretches (see Figure 10). Mass spectra of the polymers do not show individual monomer units but do show envelopes up to 370 amu for polyethylborazylene, **XI**, and 460 amu for polypropylborazylene, **XII** (Figure 11). However, they do show loss of alkyl groups, 29 amu for ethyl groups and 43 amu for propyl groups, from individual fragment peaks. Masses above 400 amu corresponding to a $(B_3N_3H_3(C_3H_7))_4$ fragment are seen for the propyl polymer and above 300 amu, corresponding to a $(B_3N_3H_3(C_2H_5))_3$ fragment, for the ethyl polymer. The ^1H NMR spectra of poly(*B*-alkylborazylenes) show broad resonances around 1 ppm due to the alkyl groups and broadened resonances between 3.5 and 6.0 ppm from the overlapping B–H and N–H resonances. Their ^{11}B NMR spectra have broad resonances at 30 and 36 ppm arising from ring the B–H and B–alkyl borons. Elemental analysis of the *B*-alkylborazine polymers synthesized at 70 °C indicate empirical formulas $B_3N_{3.5}H_{3.0}(C_2H_5)_{1.0}$ for poly(ethylborazylene) and $B_3N_{2.9}H_{2.7}(C_3H_7)_{1.0}$ for poly(propylborazylene), close to those expected for alkylborazine polymers resulting from the dehydropolymerization of *B*-alkylborazines, $(B_3N_3H_3R)_x$.

Molecular weight studies of the polymerized *B*-alkylborazines indicate that these polymers have M_n similar to the parent polymer, M_n = 540 for polyethylborazylene, and M_n = 468 for polypropylborazylene. However, M_w are considerably less than the parent polymer, M_w = 926 for polyethylborazylene and M_w = 824 for polypropylborazylene. This is consistent with the formation of fewer cross-links between polymers, as would be expected given that one of the B–H groups has been removed. Likewise, the presence of a greater number of short linear chains in the poly(*B*-alkylborazylenes) relative to the parent polyborazylene could also contribute to the molecular weight reduction.

The polyalkylborazylenes were obtained as clear viscous materials. They were soluble in a variety of solvents such as chloroform, methylene chloride, and

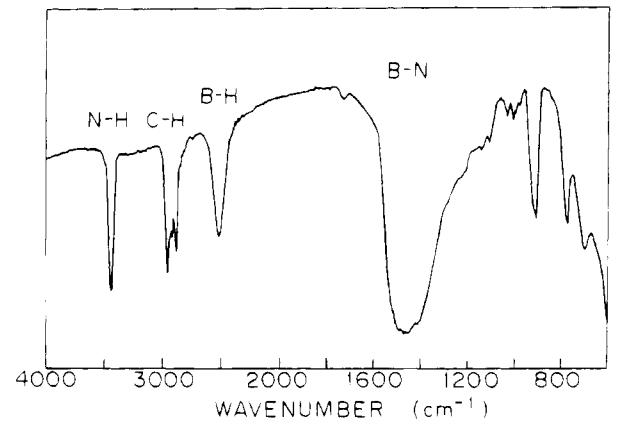

Figure 10. Infrared spectrum of poly(*B*-ethylborazylene).

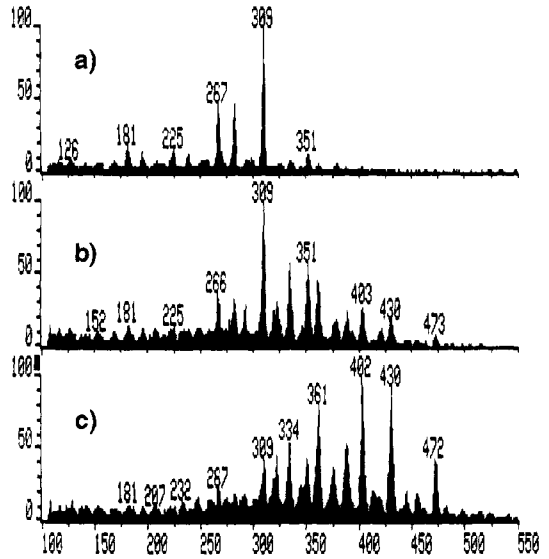

Figure 11. Mass spectra of poly(*B*-propyl)borazylene, **XII**, heated to successively higher temperatures [(a) → (b) → (c)].

benzene. Due to their high solubilities, density measurements could not be obtained using halocarbons.

When *B*-ethylborazine was heated at 90 °C, the polymerization was complete in 1 week. Again, the polymerization did not form opaque solids as with borazine. However, *B*-alkylborazines polymerized at 90 °C appeared to partially fragment, as elemental analysis indicates the boron to carbon ratio was higher in the polymer, ~2:1, than in the alkylborazine, 3:2, with an empirical formula of $B_3N_{3.1}H_{2.5}(C_2H_5)_{0.7}$, **X.** This suggests that some alkyl groups are lost during polymerization. This polymer did show higher molecular weights, with M_n = 786 and M_w = 3200, than the polyalkylborazylenes synthesized at 70 °C.

The second method by which *B*-alkylpolyborazylene polymers were produced was by the $RhH(CO)(PPh_3)_3$ catalyzed hydroboration of olefins with polyborazylene (eq 8), as described previously.[20]

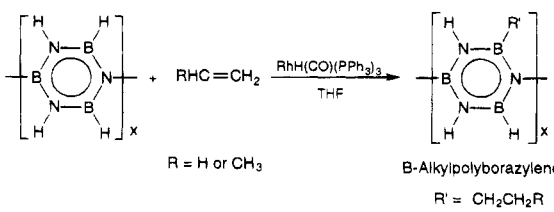

(8)

The degree of alkylation, determined by the carbon-to-boron ratio in the elemental analysis, of the alkylated polyborazylene varied. The highest degree of alkylation was slightly more than one alkyl group for every borazine ring in ethyl-substituted polymer, $B_3N_{3.2}H_{2.4}(C_2H_5)_{0.9}$ (**XIII**), and less than one alkyl group per every two rings for the propyl-substituted polymer, $B_3N_3H_3(C_3H_7)_{0.4}$ (**XIV**).

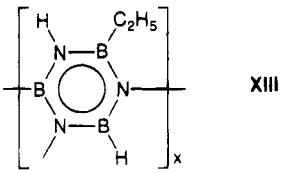

XIII

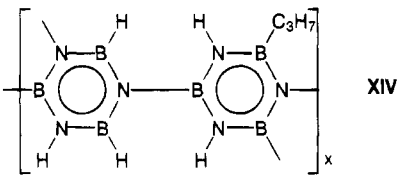

XIV

Molecular weight studies showed increased molecular weights, M_n = 1349, compared to the crude starting polymer (M_n = 506) with incorporation of ethyl groups into the polymer. Again, since these samples were precipitated, the more soluble lower weight oligomers may have been removed during this step, enhancing the portion of less soluble, higher molecular weight species. However, this was not always the case as observed for the propyl-substituted polymer, **XII**, with M_n = 608. Density measurements indicate that these polymers are less dense (1.42 g/mL) than the parent polymer. Infrared spectra of these polymers are similar to those of the polymerized *B*-alkylborazines discussed above.[20] Their ^{11}B NMR spectra were extremely broad and featureless.

Ceramic Conversion Reactions. *Bulk Pyrolysis Reactions.* Because of its composition, having only to lose hydrogen to form boron nitride, high yield synthesis, and excellent solubility in ethers, polyborazylene appeared to be an ideal chemical precursor to boron nitride. Indeed, bulk pyrolyses of the polymer under either argon or ammonia to 900–1450 °C were found to result in the formation of white, boron nitride powders in excellent chemical (89–99%) and ceramic yields (85–93%, theoretical ceramic yield, 95%). The results of the bulk pyrolytic studies are summarized in Table 2:

$$[B_3N_3H_{\sim 4}]_x \xrightarrow{25-1200\ ^\circ C} 3BN + 2H_2 \qquad (9)$$

Elemental analysis of all powder samples showed boron and nitrogen ratios of ~1:1. None of the samples contained detectable amounts of hydrogen. This is of importance since trace amounts of hydrogen can seriously affect the stability and properties of the ceramic product. The analytical results are likewise consistent with the diffuse reflectance infrared (DRIFT) spectra (Figure 12) which showed no bands near 3400 or 2500 cm^{-1}, indicating no N–H or B–H fragments were present in the samples. The observed B–N absorptions are consistent with those previously reported for hexagonal boron nitride.[37]

One sample, **D**, the precipitated polymer pyrolyzed under ammonia at 900 °C, was found to contain trace amounts of carbon. This probably resulted from solvent

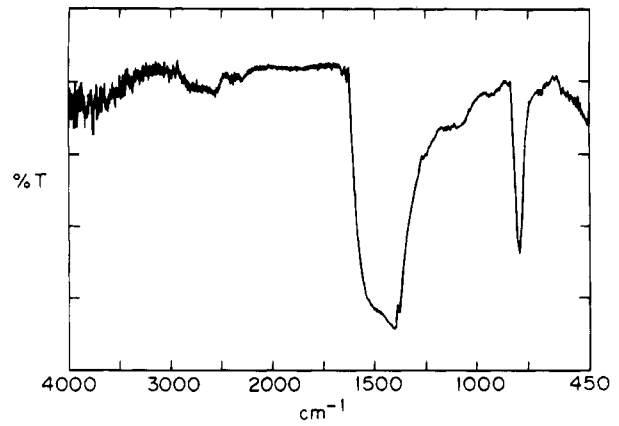

Figure 12. DRIFT spectrum of boron nitride produced from polyborazylene at 1450 °C.

retained during the precipitation.

As shown in Table 3, the pyrolysis temperature affected the properties of the boron nitride product. The X-ray powder diffraction spectra of all samples showed the presence of turbostratic BN,[38] and increasing the pyrolysis temperatures increased the crystallinity of the samples as evidenced by the shift in the 002 peak near 26° 2θ to lower values, approaching the 3.33 Å value observed for hexagonal boron nitride.[39] Likewise, as the pyrolysis temperatures were increased, the diffraction peaks progressively sharpened. Samples produced at 900 °C show broad peaks, including the (002) reflection, and the unresolved (001), (101) doublet near 42° 2θ. However, samples prepared at 1450 °C show considerably sharper peaks and resolution of the (004) reflection near 54° 2θ (Figure 13). Consistent with the XRD measurements, as the pyrolysis temperature was increased, the densities of the boron nitride samples increased from 1.7 to 2.0 g/cm^3.

The quality of the boron nitride ceramic product produced from a polymeric precursor may be best assessed by its resistance to oxidation at high temperature. This property is important for the use of boron nitride in a number of applications, particularly as a protective coating on carbon. Pure boron nitride does not oxidize in air until above 800 °C,[40] but impurities can significantly lower this temperature. The boron nitride produced from polyborazylene showed excellent resistance to oxidation, as shown in Figure 14. TGAs in air show no weight change for any of the samples until above 900 °C, at which point the weight increased rapidly due to the formation of boron oxides. Above 1100 °C a weight loss began with the vaporization of B_2O_3. Increasing the ceramic pyrolysis temperature did not significantly affect the onset of oxidation for samples produced under ammonia. However, the crude polymer samples pyrolyzed at 900 °C showed the onset of oxidation just below 900 °C, while those pyrolyzed at

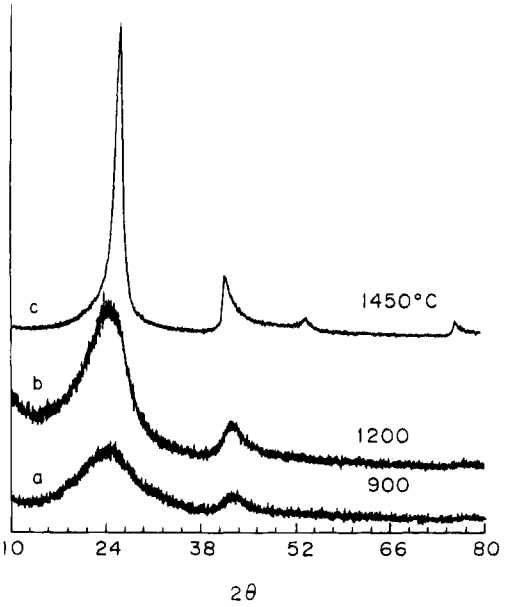

Figure 13. XRD patterns of boron nitride produced from polyborazylene under argon at (a) 900, (b) 1200, and (c) 1450 °C.

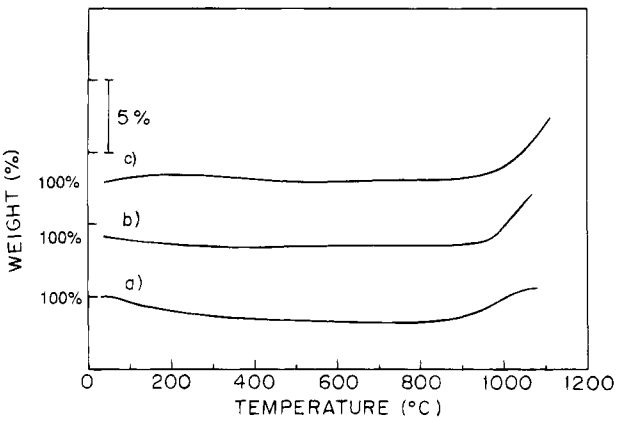

Figure 14. TGA in air of boron nitride produced from pyrolysis of polyborazylene under argon at (1) 900, (b) 1200, and (c) 1450 °C.

higher temperatures showed onset temperatures above 900 °C.

Preceramic polymers offer a number of advantages for producing ceramics in processed forms, such as fibers, coatings, and shaped objects, that are needed for many technological applications. Polyborazylene, because of its solubility, low-temperature decomposition, and high ceramic and chemical yields, appears to be ideally suited for many of these purposes. One potential use of particular importance is for the generation of boron nitride fiber coatings in ceramic and carbon composites. A boron nitride coating can enhance the toughness of a ceramic fiber composite by both reducing crack propagation and increasing the potential for fiber pullout.[41] Boron nitride coatings on carbon fiber can also provide protection against oxidation.

Preliminary fiber coating studies with polyborazylene were carried out by simply dipping fiber bundles in dilute solutions (1−10% w/w) of the polymer dissolved

(37) (a) Brame, E. G., Jr.; Margrave, J. L.; Meloche, V. W. *J. Inorg. Nucl. Chem.* **1957**, *5*, 48−52. (b) Rand, M. J.; Roberts, J. F. *J. Electrochem. Soc.* **1968**, *115*, 423−429. (c) Takahashi, T.; Itoh, H.; Takeuchi, A. *J. Cryst. Growth* **1979**, *47*, 245−250.

(38) (a) Pease, R. S. *Acta Crystallogr.* **1952**, *5*, 356−361. (b) Thomas, J., Jr.; Weston, N. E.; O'Connor, T. E. *J. Am. Chem. Soc.* **1963**, *84*, 4619−4622. (c) Economy, J.; Anderson, R. *Inorg. Chem.* **1966**, *5*, 989−992. (d) Matsuda, T.; Uno, N.; Nakae, H.; Hirai, T. *J. Mater. Sci.* **1986**, *21*, 649−658.

(39) *Gmelin Handbuch der Anorganischen Chemie, Boron Nitride. B-N-C Heterocyles. Polymeric B-N Compounds;* Springer-Verlag: New York, 1974; Vol. 13, Part 1; pp 1−87.

(40) Alekseev, A. F.; Lavrenko, V. A.; Neshpor, V. S.; Frantsevich, I. N. *Dokl. Akad. Nauk. SSSR* **1978**, *238*, 370−373.

(41) See, for example: (a) Singh, R. N.; Brun, M. K. *Ceram. Eng. Sci. Proc.* **1987**, *8*, 636−643. (b) Freeman, G. B.; Lackey, W. J. *Pro. Annu. Meet. Electron Microsc. Soc. Am., 46th* **1988**, 740−741. (c) Brun, M. K.; Singh, R. N. *Adv. Ceram. Mater.* **1988**, *3*, 506−509. (d) Singh, R. N.; Brun, M. K. *Adv. Ceram. Mater.* **1988**, *3*, 235−237.

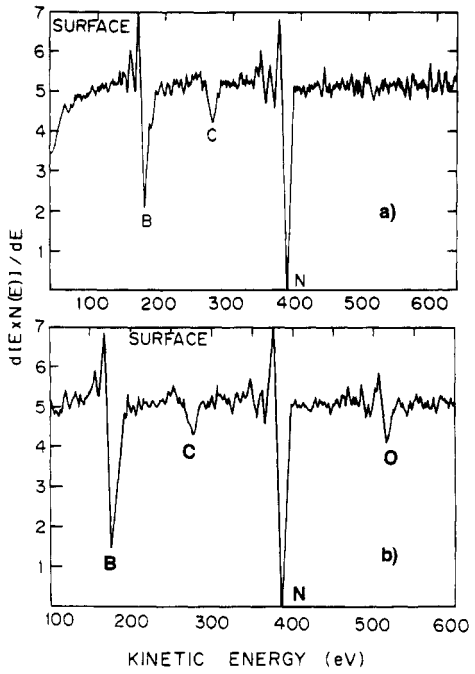

Figure 15. AES of boron nitride coated (a) alumina ceramic fiber and (b) carbon fiber.

in THF or glyme. The solvent was then evaporated to give a polymer-coated fiber. The polymer coated fibers were then pyrolyzed to >900 °C in a tube furnace under argon to give boron nitride coated materials. The best coatings appeared to be produced with 3–7% w/w polymer solutions. Excellent coatings were produced on a variety of fibers and typical AES spectra obtained from boron nitride coated carbon (P-55) and Al_2O_3/ZrO_2 (PRD-166) fibers are shown in Figure 15a.

Economy and Kim[42] have also reported using viscous liquid polyborazylene samples from which the volatile lower molecular weight species (including unreacted borazine, borazanaphthalene and diborazine) had not been separated, for producing a carbon fiber/boron nitride matrix composites. The resulting boron nitride matrices showed a significant increase in oxidative stability over carbon matrices. Other recent examples of polyborazylene applications include its use for the formation of boron nitride thin films on silicon wafers[43] and its use as a reagent for the synthesis of titanium-boride/titanium-nitride composites.[44]

Ceramic Conversion Reaction. The polyborazylene ceramic conversion reaction was also studied in more detail with a number of techniques to gain insight into the steps involved in the polymer-to-ceramic conversion. As we reported previously,[17] thermogravimetric studies of the polyborazylene-to-boron nitride conversion reaction showed that the polymer undergoes a two-stage weight loss as shown in Figure 16. An initial (2%) weight loss is observed in a narrow range between 125 and 300 °C. Over a broad range, between 300 and 700 °C, minimal weight loss is observed. Weight loss resumes at 700 °C, continuing to above 1100 °C with a

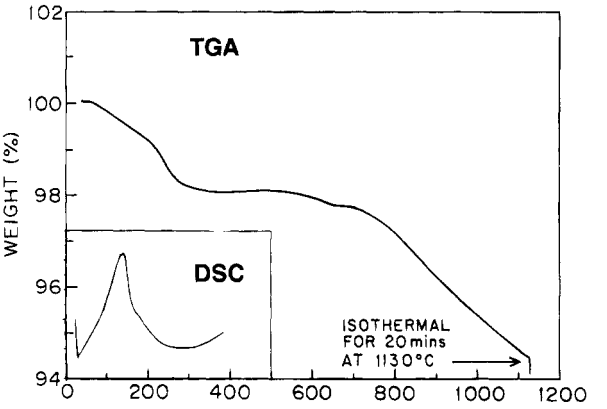

Figure 16. TGA of polyborazylene under argon. DSC of polyborazylene (inset).

gradual 4% loss. During this latter stage elementally pure turbostratic boron nitride is produced. TGA studies of all samples showed similar 2-stage weight losses at comparable temperatures, but the percent weight loss at each step varied depending on the particular polymer sample. Consistent with the TGA results, a differential scanning calorimetry study (over the range of 25–400 °C) showed a large exotherm starting below 50 °C continuing to around 300 °C (Figure 16, inset).

A combined TGA/MS study was then used to determine the identity of the evolved species at each step. Hydrogen loss was clearly the dominant component of the observed losses at all temperatures for all polymer samples, but small amounts of a number of boron containing species were observed, by mass spectrometry, to evolve from the crude polymers during the early stages of the conversion reaction. Thus, below 300 °C, small amounts of species with approximate masses of 2, 80, 96, 105, and 131 were observed to evolve from the crude polymers. Species with m/z = 80 and 131 correspond to borazine and borazanaphthalene, respectively. Above 300 °C these species cease to evolve. TGA/MS studies of the pyrolysis of the precipitated polymers indicate that no boron-containing species with m/z < 200 were evolved. The only species seen above 300 °C in either the crude or precipitated polymers was hydrogen. Hydrogen evolution peaks between 500 and 700 °C, corresponding to the second weight-loss step observed in the TGA. Consistent with these results, it was found that crude polymer samples gave somewhat lower ceramic yields, probably due to the fact that the lower molecular-weight oligomers contained in the crude polymer samples may sublime out during the pyrolysis. Likewise, it was found that the ceramic yields were greatest for the higher molecular weight samples. TGA studies of the series of polymers in Figure 17 showed that the sample polymerized for 48 h had the smallest weight loss of the three samples, 13% overall. Samples prepared for 36 and 22 h showed 17.5% and 22% overall weight losses, respectively. This trend may be due to the lower hydrogen content of the samples and/or the presence of higher concentrations of higher molecular weight species in samples polymerized for longer periods. Higher molecular weight species are less volatile and should form interchain cross-links before any volatilization occurs.

To obtain information on the nature of the species present during the intermediate stages of the ceramic conversion reaction, a bulk sample of polyborazylene was heated to a temperature (400 °C) that was just

(42) (a) Kim, D.-P.; Economy, J. *Chem. Mater.* **1993**, *5*, 1216–1220. (b) Kim, D.-P.; Economy, J. *Ceram. Trans.* **1993**, *38*, 47–52.
(43) Chan, V. Z.-H.; Composto, R. J.; Rothman, J. B.; Sneddon, L. G. Materials Research Society Meeting, Boston, November 1994.
(44) (a) Su, K.; Nowakowski, M.; Bonnell D; Sneddon; L. G. *Chem. Mater.* **1992**, *31*, 1139–1141. (b) Nowakowski, M.; Su, K.; Sneddon; L. G.; Bonnell, D. *Mater. Res. Soc. Proc.* **1993**, *286*, 425–430. (c) Szabo, V.; Nowakowski, M.; Su, K.; Sneddon; L. G.; Ruhle, M.; Bonnell D. *Mater. Res. Soc. Proc.* **1993**, *286*, 431–440.

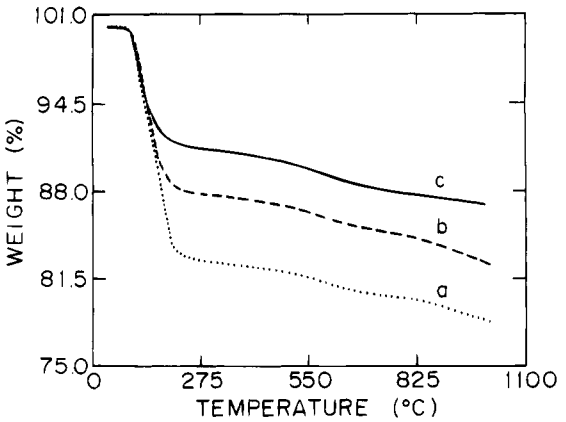

Figure 17. TGA of polyborazylene polymers produced by heating borazine for (a) 22, (b) 36, and (c) 48 h.

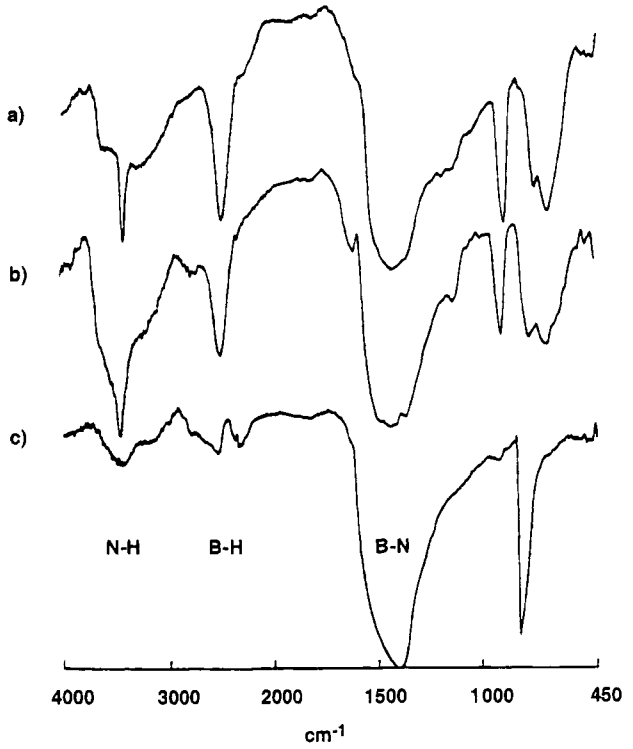

Figure 18. Diffuse-reflectance infrared spectra of (a) polyborazylene, (b) polyborazylene heated to 400 °C, and (c) boron nitride produced at 1450 °C.

beyond the temperature range (125–300 °C) of the first major weight loss observed in the TGA and the product analyzed. Elemental analysis of the resulting white powder showed an empirical formula of $B_3N_3H_{\sim 2}$. The near 1:1 boron:nitrogen ratio but smaller hydrogen content found for this product relative to the polyborazylene is consistent with the TGA results discussed above which demonstrated that hydrogen loss is the dominant process observed at all stages of the ceramic conversion. These results suggest that at this stage the ceramic conversion reaction involves interchain polymer cross-linking. As expected for a cross-linked material, the 400 °C material showed an increased density (1.75 g/mL) compared to the starting polymer (1.56 g/mL) and was insoluble in a variety of polar solvents. The DRIFT spectra of polyborazylene, the 400 °C material, and the boron nitride product (Figure 18) show progressive decreases in both the B–H and N–H stretching intensities as the the polymer is heated to 1450 °C. This suggests that as the temperature is increased, both the B–H and N–H groups are reacting at reasonably

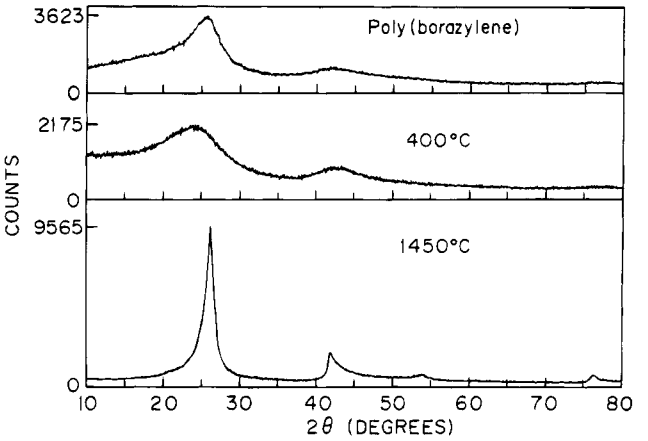

Figure 19. Powder XRD of (a) polyborazylene, (b) polyborazylene heated to 400 °C, and (c) boron nitride produced at 1450 °C.

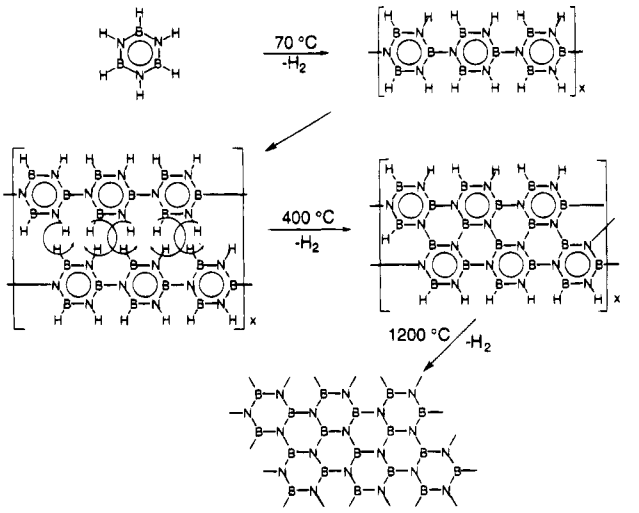

Figure 20. Possible polymer/ceramic conversion process of polyborazylene.

comparable rates and implies the increasing formation of boron–nitrogen cross-links until the final boron nitride structure is achieved.

X-ray diffraction studies of polyborazylene and the 400 °C intermediate material showed that both materials exhibit patterns similar to those observed for turbostratic boron nitride (Figure 19). Thus, both spectra show very broad peaks near 26° and 42° 2θ, where the (002) and (10) lines appear in boron nitride (Figure 13). These observations suggest that the layered structure of boron nitride is already present in the polymer in the solid state and that this layer structure is preserved during the conversion to boron nitride. The presence of a layer structure is also consistent with the observed small density change that is observed when the polymer (1.56 g/mL) is converted to the 400 °C material (1.75 g/mL) and then to the ceramic (1.7–2.0 g/mL). The above observations are also consistent with the report by Kim and Economy that layered liquid crystalline mesophases form when viscous polyborazylene solutions are allowed to sit at 0–5 °C for extended times.[28]

The combined spectroscopic and crystallographic studies discussed above suggest a simple process for the polyborazylene to boron nitride conversion. As can be seen in Figure 20, if two polyborazylene chains with an *idealized* linear structure are brought together in the manner shown, they are in position to undergo interchain dehydrocoupling reactions to yield a B–N cross-

linked material. In this sequence the structure of boron nitride may be formed by a 2-dimensional process without disrupting the interlayer spacing. On the basis of the simple process depicted in the figure, it might be expected that only a one-step, low-temperature weight-loss reaction would be required to form boron nitride. However, the TGA experiments indicate that the conversion to boron nitride occurs in two stages, with an initial loss between 125 and 300 °C followed by a second loss between 700 and 1100 °C. This behavior is, however, consistent with the fact that the polymer is known from the molecular weight studies discussed earlier to not have the idealized linear structure depicted in the Figure, but rather to have a extensively chain-branched structure. In such a chain branched structure it would not be possible to have complete alignment of the polymer chains. Thus, the initial hydrogen loss observed over the 125−300 °C range may well be due to dehydro-cross-linking of B−H and N−H groups on adjacent chains, but the higher temperature process occurring over the 700−1100 °C range is probably required to induce hydrogen loss from the unaligned chain branches, ultimately then forming the boron nitride ceramic. It should be noted that this two-stage conversion is, in fact, promising for many technological applications where the polymer must be shaped to a desired form and then cross-linked at relatively low temperatures.

As mentioned earlier, the low-temperature cross-linking stage found for the parent polyborazylene polymer limits the use of the parent polymer for applications, such as for forming melt-spun fibers, where a polymer melt needs to be employed. For these purposes it will be necessary to design and synthesize "second-generation" polyborazylene polymers in which the cross-linking reactions, as well as other polymer properties, such as solubility, may be systematically controlled. Our discovery that alkyl-substituted polyborazylenes may be readily produced either by the thermal polymerization of *B*-alkylborazines or by the transition-metal-catalyzed polyborazylene/olefin hydroboration reaction demonstrates that a range of substituted polyborazylene polymer systems should now be possible. Significantly, TGA studies (Figure 21a,b) of these two polymers under argon show that the onset of the intial weight loss is at higher temperatures than the parent polymer suggesting that alkyl groups do, in fact, inhibit the interchain dehydrocoupling. Both polymers, however, show larger weight losses during pyrolysis than polyborazylene. If the weight losses were due only to loss of the alkyl groups and hydrogen, then the predicted ceramic yields of BN for the *B*-alkylpolyborazylenes would be between 72 and 80% which is close to those that were observed. For the poly-*B*-alkylborazylenes, predicted ceramic yields based on loss of only the alkyls and hydrogen would be 72% for the ethyl polymer and

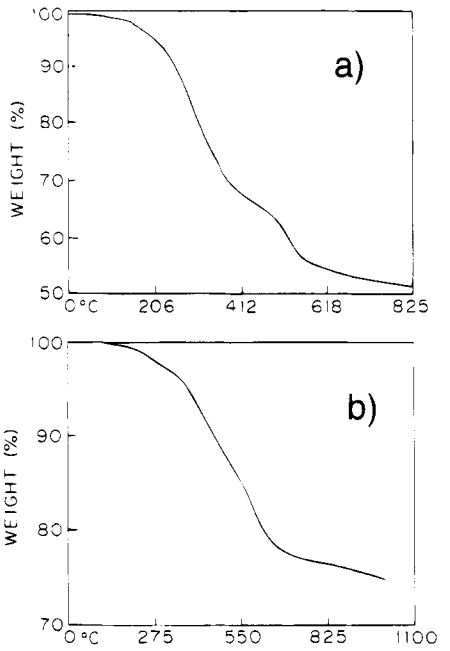

Figure 21. TGA of (a) poly(*B*-ethylborazylene) and (b) *B*-ethyl-polyborazylene.

63% for the propyl polymer, but both polymers showed ceramic yields of near 50%. The lower yield was probably due to volatilization of lower molecular-weight species, since TGA/MS studies of these polymers show, in addition to hydrogen and hydrocarbons, the loss of some alkylborazine species. The final stages of weight loss in both polymers again appear to be due to loss of hydrogen.

The initial studies of the alkylated polyborazylenes clearly demonstrate that systematic modification of the polyborazylene polymer is possible and that such modification can be used to control the polymer properties. We are now exploring the synthesis and materials applications of a range of new polymer series based on the polyborazylene framework and these will be reported in future publications.

Acknowledgment. We thank the U.S. Department of Energy, Division of Chemical Sciences, Office of Basic Energy Sciences, Office of Energy Research, and the National Science Foundation Materials Research Laboratory at the University of Pennsylvania for their support of this research. We also thank Mr. Bruce Rothman for his assistance with the Auger results.

Supporting Information Available: Tables for diborazine and borazanaphthalene listing refined thermal parameters, bond distances, bond angles, calculated hydrogen atom positions, and least-squares planes (11 pages); a listing of observed and calculated structure factors (10 pages). Ordering information is given on any current masthead page.

CM950230Q